Implementation of the Negative Moment Reinforcing Detail Recommendations

Final Report
April 2021

IOWA STATE UNIVERSITY
Institute for Transportation

Sponsored by
Iowa Highway Research Board
(IHRB Project TR-723)
Iowa Department of Transportation
(InTrans Project 17-606)

About the Bridge Engineering Center

The mission of the Bridge Engineering Center (BEC) is to conduct research on bridge technologies to help bridge designers/owners design, build, and maintain long-lasting bridges.

About the Institute for Transportation

The mission of the Institute for Transportation (InTrans) at Iowa State University is to save lives and improve economic vitality through discovery, research innovation, outreach, and the implementation of bold ideas.

Iowa State University Nondiscrimination Statement

Disclaimer Notice

Iowa DOT Statements

The preparation of this report was financed in part through funds provided by the Iowa Department of Transportation through its "Second Revised Agreement for the Management of Research Conducted by Iowa State University for the Iowa Department of Transportation" and its amendments.

Technical Report Documentation Page

1. Report No.	2. Government Accession No.	3. Recipient's Catalog No.
IHRB Project TR-723		

4. Title and Subtitle	5. Report Date
Implementation of the Negative Moment Reinforcing Detail Recommendations	April 2021
	6. Performing Organization Code
7. Author(s)	**8. Performing Organization Report No.**
Katelyn S. Freeseman (orcid.org/0000-0003-0546-3760), Zhengyu Liu (orcid.org/0000-0002-7407-0912), and Brent M. Phares (orcid.org/0000-0001-5894-4774)	InTrans Project 17-606
9. Performing Organization Name and Address	**10. Work Unit No. (TRAIS)**
Bridge Engineering Center Iowa State University 2711 South Loop Drive, Suite 4700 Ames, IA 50010-8664	**11. Contract or Grant No.**
12. Sponsoring Organization Name and Address	**13. Type of Report and Period Covered**
Iowa Highway Research Board Iowa Department of Transportation 800 Lincoln Way Ames, IA 50010	Final Report
	14. Sponsoring Agency Code

15. Supplementary Notes

Visit https://intrans.iastate.edu/ for color pdfs of this and other research reports.

16. Abstract

It is common practice to put additional longitudinal reinforcement (b2 bars) over intermediate supports to resist any negative moment induced by the superimposed dead loads and live loads on bridges. However, little research has been conducted on the performance of the additional negative reinforcing steel. Requirements for the termination of the additional negative moment reinforcing steel have largely been based on engineering judgement, previous performance, and existing practice.

The main objective of this research was to evaluate the effect of different amounts of b2 bar on resisting the negative moment over the pier on a continuous prestressed concrete girder bridge when it is subject to the live load-generated moment and secondary moment. To achieve this objective, a live load field test was performed on a bridge designed with different amounts of b2 bars to allow for comparison of the varying levels of negative moment reinforcement present.

A full-scale finite element model was developed and validated against the field-collected data to study b2 bar performance subjected to live loads. An evaluation was performed utilizing an analytical approach by calculating the time-dependent secondary moment using mRESTRAINT and loading the beam-line finite element model with the maximum negative moment.

It was found that the negative moment induced by the live load and secondary moment does appear through the service life of the bridge. The high differential shrinkage rate between the fresh deck concrete and the girder concrete is the main source of the negative moment over the supports. The magnitude of the secondary moment was found to be highly influenced by the time when the continuity is established.

The results also indicated that the additional longitudinal reinforcing steel provides minimal effect on resistance to the negative moment prior to the formation of deck cracking, regardless of whether the negative moment was induced by live loads or by the secondary moment. The current design approach determines the b2 bar requirement for the strength level based on the live load, while it may be necessary to include the secondary moment in the design.

17. Key Words	18. Distribution Statement
bridge decks—field testing—finite element models—negative moment reinforcement—secondary moment	No restrictions.

19. Security Classification (of this report)	20. Security Classification (of this page)	21. No. of Pages	22. Price
Unclassified.	Unclassified.	49	NA

Form DOT F 1700.7 (8-72) **Reproduction of completed page authorized**

IMPLEMENTATION OF THE NEGATIVE MOMENT REINFORCING DETAIL RECOMMENDATIONS

Final Report
April 2021

Principal Investigator
Brent M. Phares, Research Associate Professor
Bridge Engineer Center, Iowa State University

Co-Principal Investigator
Katelyn Freeseman, Associate Director
Bridge Engineer Center, Iowa State University

Research Assistant
Zhengyu Liu, Research Engineer
Bridge Engineer Center, Iowa State University

Authors
Katelyn Freeseman, Zhengyu Liu, and Brent M. Phares,

Sponsored by
Iowa Highway Research Board and
Iowa Department of Transportation
(IHRB Project TR-723)

Preparation of this report was financed in part
through funds provided by the Iowa Department of Transportation
through its Research Management Agreement with the
Institute for Transportation
(InTrans Project 17-606)

A report from
Bridge Engineering Center
Institute for Transportation
Iowa State University
2711 South Loop Drive, Suite 4700
Ames, IA 50010-8664
Phone: 515-294-8103 / Fax: 515-294-0467
https://intrans.iastate.edu/

TABLE OF CONTENTS

ACKNOWLEDGMENTS vii

EXECUTIVE SUMMARY ix

CHAPTER 1. INTRODUCTION 1

- 1.1 Background 1
- 1.2 Objective and Approach 2
- 1.3 Research Plan 2

CHAPTER 2. LITERATURE REVIEW 3

CHAPTER 3. FIELD EVALUATION 5

- 3.1 Bridge Selection and Negative Moment Reinforcement Design 5
- 3.2 Live Load Application and Instrumentation Plan 8
- 3.3 Live Load Test Results 11
  - 3.3.1 2018 Test 11
  - 3.3.2 2019 Test 14
  - 3.3.3 2020 Test 18
  - 3.3.4 Field Test Results Discussion 21
- 3.4 Field Inspection 22

CHAPTER 4. ANALYTICAL STUDY 24

- 4.1 Full-Scale Model 24
  - 4.1.1 Model Development 24
  - 4.1.2 Model Validation 26
  - 4.1.3 Effect of B2 Bars 30
- 4.2 Calculation of Secondary Moment 31
- 4.3 Small-Scale Model 35
  - 4.3.1 Model Development 35
  - 4.3.2 Results 35

CHAPTER 5. CONCLUSION AND RECOMMENDATIONS 37

- 5.1 Conclusions 37
- 5.2 Recommendations and Future Research Directions 38

REFERENCES 39

LIST OF FIGURES

Figure 1 Timeline for bridge construction, deck crack inspections, and live load tests 5
Figure 2. Newly constructed bridge on E-57 over I-35 6
Figure 3. E-57 over I-35 bridge drawings...7
Figure 4. Truck information...8
Figure 5. Load and instrumentation plan (plan view) 9
Figure 6. BDI gauges instrumentation (cross-section view)...10
Figure 7. Field instrumentation...10
Figure 8. 2018 deck strain data (LC2) 12
Figure 9. 2018 strain data at bottom flange (LC2)..13
Figure 10. 2018 strain data at top flange (LC2)..14
Figure 11. 2019 deck strain data (LC2) 15
Figure 12. 2019 BDI strain data at bottom flange (LC2)...16
Figure 13. 2019 BDI strain data at top flange (LC2)...17
Figure 14. 2020 deck strain data (LC2) 19
Figure 15. 2020 strain data at bottom flange (LC2)..20
Figure 16. 2020 strain data at top flange (LC2)..21
Figure 17. Data comparison over the years 22
Figure 18. Bridge deck top surface 23
Figure 19. Full-scale bridge model 25
Figure 20. Validation by deck strain data (LC2) 27
Figure 21. Validation by BDI strain data at bottom flange (LC2)...28
Figure 22. Validation by BDI strain data at top flange (LC2) 29
Figure 23. Deck top stress-induced-strain over Pier 1 and 2 30
Figure 24. Deck top stress-induced-strain over Pier 3 and 4 31
Figure 25. Secondary moment development-1 33
Figure 26. Secondary moment development-2 34
Figure 27. Maximum stress-induced-strain on top of deck 35
Figure 28. Deck stress-induced-strain comparison between the models with and without negative moment reinforcement...36

LIST OF TABLES

Table 1. Material properties..25
Table 2. Pre-stressed precast girder data...32
Table 3. Parameters used to calculate secondary moment 32

ACKNOWLEDGMENTS

The research team would like to acknowledge the Iowa Highway Research Board (IHRB) and Iowa Department of Transportation (DOT) for sponsoring this research.

The authors would also like to thank Ayman M. Okeil and his research team at Louisiana State University for support of this research by providing the software program, mRESTRAINT, and the original developers of RESTRAINT, Richard A. Miller and his team.

EXECUTIVE SUMMARY

It is common practice to put additional longitudinal reinforcement (b2 bars) over intermediate supports to resist negative moment induced by the superimposed dead loads and live loads on bridges. However, little research has been conducted on the performance of and need for the additional negative reinforcing steel. Requirements for the termination of the additional negative moment reinforcing steel have largely been based on engineering judgement, previous performance, and existing practice.

The main objective of this research was to evaluate the effect of different amounts of b2 bar on resisting the negative moment over the pier on a continuous prestressed concrete girder bridge when it is subject to the live load-generated moment and secondary moments. To achieve this objective, a live load field test was performed on a bridge designed with different amounts of b2 bars to allow for comparison of the varying levels of negative moment reinforcement present. A full-scale finite element model was developed and validated against the field-collected data to study b2 bar performance subjected to live loads. An evaluation was performed utilizing an analytical approach by calculating the time-dependent secondary moment using mRESTRAINT and loading the beam-line finite element model with the maximum negative moment.

It was found that the negative moment induced by the live load and secondary moment does appear through the service life of the bridge. The high differential shrinkage rate between the fresh deck concrete and the girder concrete is the main source of the negative moment over the supports. The magnitude of the secondary moment was found to be highly influenced by the time when the continuity is established.

The results also indicated that the additional longitudinal reinforcing steel provides minimal effect on resistance to the negative moment prior to the formation of deck cracking, regardless of whether the negative moment was induced by live loads or by the secondary moment. The current design approach determines the b2 bar requirement for the strength level based on the live load, while it may be necessary to include the secondary moment in the design. Further, current design approaches for the amount of b2 bars may be overly conservative.

CHAPTER 1. INTRODUCTION

1.1 Background

Pre-stressed concrete girder bridges have historically been designed with negative moment reinforcement in order to resist loads after full continuity is achieved. The Iowa Department of Transportation (DOT) Office of Bridges and Structures Bridge Design Manual specifically calls for additional longitudinal, so called b2, bars for resistance to negative moments caused by super-imposed dead loads and live loads.

In an attempt to determine if current negative moment reinforcement requirements are overly conservative, a previous study performed by the Bridge Engineering Center at Iowa State University found that the amount of b2 reinforcement for negative moment regions of pre-stressed girder bridges may not be needed to the level currently specified (Phares et al. 2015). This finding is particularly important because current design approaches were indicating that increasing amounts of reinforcement were needed, causing both construction difficulties and increasing overall bridge costs.

Requirements for the termination of negative moment reinforcing steel have largely been based on judgement, previous performance, and existing practice. These requirements also vary from state to state. Additionally, work for the Federal Highway Administration (FHWA) has shown that it is possible to have secondary positive moments that offset the negative moments experienced over piers, thus resulting in no negative moment at all. These contradicting viewpoints served as the motivation behind a study performed by the Bridge Engineering Center in which the current Iowa DOT policy regarding b2 reinforcement was investigated.

This study involved the live load testing of a number of bridges, with the results used to calibrate finite element models (FEMs). The finite element results suggested that the transverse field cracks over the pier and at 1/8 of the span length are mainly due to deck shrinkage (Phares et al. 2015). In addition, it was concluded that secondary moments affect the behavior in the negative moment region. The results of this previously funded research were recommended for implementation such that further evaluations could be completed to confirm the findings and result in the development of updated requirements for negative moment reinforcement in multi-span pre-stressed concrete beam bridges.

By summarizing the background above, the following questions were found to be significant:

1. Is there any negative moment over the bridge pier?
2. Does this negative moment have a significant effect on the bridge structure and need to be considered for the design?
3. Is b2 reinforcing steel effective at resisting negative movement, and how much b2 reinforcing steel is required?
4. What type of loading should the b2 bars be designed for?

The research was conducted to answer these questions. The questions should be answered in the listed sequence such that only when one question was answered to be “yes” the next question need be answered.

1.2 Objective and Approach

The main objective of this research is to evaluate the effect of different amounts of negative moment reinforcement (b2 bars) on resisting the negative moment over the pier on a continuous prestressed concrete girder bridge. To achieve this objective, both current b2 amounts and proposed reduced amounts were investigated by conducting a field test and analytical study. The negative moments that were studied in this research include both live load generated moment and secondary generated moments.

1.3 Research Plan

Several tasks were conducted to meet the objective of the project. These tasks were performed in close communication with a technical advisory committee (TAC) that was developed for the project. The main tasks included the following:

- Literature review
- Field test of E-57 over I-35 bridge
- Analytical study on the effect of secondary moment

At the beginning of the research, a yet-to-be-constructed bridge on E-57 over I-35 designed with different amounts of b2 bar in the deck over each pier was selected and instrumented during bridge construction. This would allow for the comparison of the behavior of cross-sections with varying amounts of negative reinforcement present to help determine what requirements are necessary in the negative moment region of pre-stressed concrete girder bridges.

The live load field test was performed after the deck concrete gained enough strength, and the test was repeated every 12 months to experimentally investigate the performance of the b2 bars regarding resistance of the negative moment due to live loads.

A full-scale FEM was developed and validated against the field-collected data to analytically study the b2 bar performance when subjected to live loads. The effectiveness of the b2 bar at resisting the negative moment induced by long-term secondary moments was evaluated utilizing an analytical approach by calculating the time-dependent secondary moment using mRESTRAINT and loading the maximum negative moment on the small-scale FEM. The small-scale FEM was developed utilizing the same approach as that used on the full-scale FEM.

CHAPTER 2. LITERATURE REVIEW

The literature review was conducted with emphasis on the findings presented in the previous study performed by Phares et al. (2015). A new search of relevant material was also conducted, although no new literature was found that directly related to this topic. The results of the literature review are summarized in this chapter.

During the bridge service life, the two main sources of the negative moment are the live load and the secondary moment. The live loads generate negative moment over the pier as a vehicle moves to the middle span. Secondary moments, including both positive moment and negative moment, are induced by the creep of the pre-stressed concrete girder and the differential shrinkage rate between the deck and girder.

It is a common practice to put additional longitudinal reinforcement over the supports for resistance to the negative moment induced by the super-imposed dead load and live load. However, little research has been conducted on the performance of the negative reinforcing steel. The current American Association of State Highway and Transportation Officials (AASHTO) Load and Resistance Factor Design (LRFD) Bridge Design Specifications (2020) provides no guidelines on the design of reinforcement at the top of the continuity connection.

Wassef et al. (2003) provided a comprehensive design example of a pre-stressed concrete girder bridge, which was intended to serve as a guide to aid bridge design engineers with the implementation of the AASHTO specifications. In the example, a conservative approach with an assumption of a fully cracked cross section was adopted to calculate the demand of the negative moment reinforcement subject to the factored external superimposed loads. Many state DOTs, including the Iowa DOT, use a similar design approach without considering the secondary moment.

Freyermuth (1969) indicated that a positive moment developed over the pier on a continuous pre-stressed concrete girder bridge when the bridge deck was placed at a young girder age. The creep effect of the girder concrete influenced by the pre-stressing force creates an upward bow on the pre-stressed concrete girder. At the same time, the higher shrinkage rate of the deck concrete induced a negative bowl effect on the girder and induced negative moment to the pier region. Often, the positive secondary moment at the intermediate supports is greater than the negative secondary moment.

Phares et al. (2015) developed and calibrated a series of FEMs on a number of bridges to investigate the effect of the negative reinforcing steel over the pier on continuous pre-stressed concrete girder bridges. The researchers concluded that secondary moments affect the behavior in the negative moment region. This impact may be significant enough such that no tensile stresses in the deck may ever be experienced. In addition, the finite element results suggested that the transverse field cracks over the pier and at 1/8 of the span length are mainly due to deck shrinkage, and the reinforcement for negative moment regions of prestressed girder bridges may not be needed to the level currently specified. These results showed good agreement with the work by Freyermuth (1969).

With respect to the quantity of the b2 reinforcing steel, the researchers found that the increasing amounts of reinforcement causes both construction difficulties and overall bridge cost increases, while reduction and termination of the additional negative reinforcing steel is in demand.

AASHTO LRFD Bridge Design Specifications (2020) require an embedment length beyond the point of inflection not less than the effective depth of the member, 12.0 times the nominal diameter of the bar, and 0.0625 times the clear span. However, Phares et al. (2015) indicated that requirements for the termination have largely been based on judgement, previous performance, and existing practice.

For example, the Iowa DOT Bridge Design Manual terminates the negative moment reinforcement at 1/8 of the span length and results in approximately 50% less than the recommended length, without experiencing significant cracks.

In addition, as part of this research involved the calculation of secondary moment development over the bridge pier, a literature search was conducted on the direction of the development of the secondary moment calculation software to select the most advanced option. The estimation of the secondary moment involves several uncertainties due to the time-dependent nature of the material, and extensive effort has been contributed to it during the past few decades.

Freyermuth (1969) developed an elastic structural analysis procedure considering monolithic behavior of the deck and girders to calculate the positive secondary moments due to creep and the negative secondary moment due to the differential shrinkage between the cast-in-place deck and the concrete girders using the formulas given in this Portland Cement Association (PCA) report. The performance of bridges designed according to this PCA method has been acceptable.

Oesterle et al. (1989) developed the Construction Technology Laboratory (CTL) method to calculate the complete time-history of the secondary moment, which is also known as the BridgeRM program. McDonagh and Hinkley (2003) developed a program (RMCalc), which repackages BridgeRM and uses the same algorithms.

Based on the PCA and CTL methods, Miller et al. (2004) developed a spreadsheet-based program called RESTRAINT to calculate the secondary moments of pre-tensioned pre-stressed concrete beam (PPCB) bridges with equal spans and limited section properties. Following that, a few modifications were made by Chebole (2011) and Hossain et al. (2014) on RESTAINT to allow more flexibility on the model geometries and account for the effect of thermal gradients. The most recent software package is the modified RESTAINT called mRESTAINT.

CHAPTER 3. FIELD EVALUATION

The main objective of the field evaluation was to experimentally study the performance of differing amounts of b2 reinforcement in the deck over the piers in resisting the negative moment induced by the live load. The field evaluation consisted of both live load field tests and deck concrete crack inspections. The live load tests were performed every 12 months, and the deck top crack inspections were performed every six months. Figure 1 shows the timeline for the schedule of the load tests and bridge inspections, and a few important events during the bridge construction.

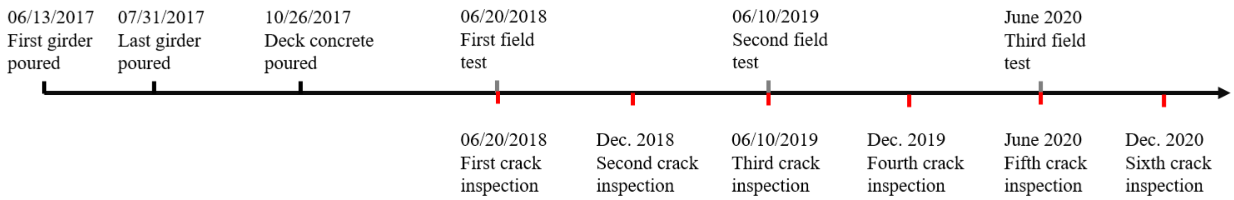

Figure 1 Timeline for bridge construction, deck crack inspections, and live load tests

The field tests also provided data for the calibration of the FEM that was developed and used in the subsequent research steps.

3.1 Bridge Selection and Negative Moment Reinforcement Design

To compare the performance of the different amounts of b2 bar and keep the other parameters (such as environment temperature and humidity, bridge age, and traffic volume) the same, a yet-to-be-constructed bridge on E-57 over I-35 was selected for the field tests and was designed with different amounts of b2 reinforcement over each pier. This bridge (Figure 2) had five spans, measuring 443 ft by 30 ft on a zero-degree skew, and was located 2 miles south of the US 30 and I-35 interchange.

Figure 2. Newly constructed bridge on E-57 over I-35

The exterior spans were 41 ft and 51 ft, and the interior spans were 117 ft (as depicted in Figure 3-a).

This bridge utilized both conventional amounts of negative moment reinforcement and reduced amounts (depicted in Figure 3-b). The b2 bars over Pier 1 and Pier 4 were designed in a conventional manner to carry 100% of the estimated negative moment based on AASHTO LRFD bridge design specifications.

The design was based on a single reinforced beam utilizing a composite cross section consisting of an interior pre-stressed beam and the associated deck tributary area. There was no attempt at including secondary moments in the loading.

The b2 bars over Pier 2 were designed based on 1% of the deck cross-sectional area. The basis for this design was the Iowa DOT’s continuously welded plate girder bridges, which currently perform well using 1% of the deck cross-sectional area for their reinforcement.

The b2 bars over Pier 3 were designed in a similar way to the b2 bars over Pier 1 and Pier 4. However, the section was designed to carry only 50% of the estimated negative moment. This resulted in different bar sizes over each pier as follows: No.9 bars over Pier 1, No.6 bars over Pier 2, No. 5 bars over Pier 3, and No. 8 bars over Pier 4.

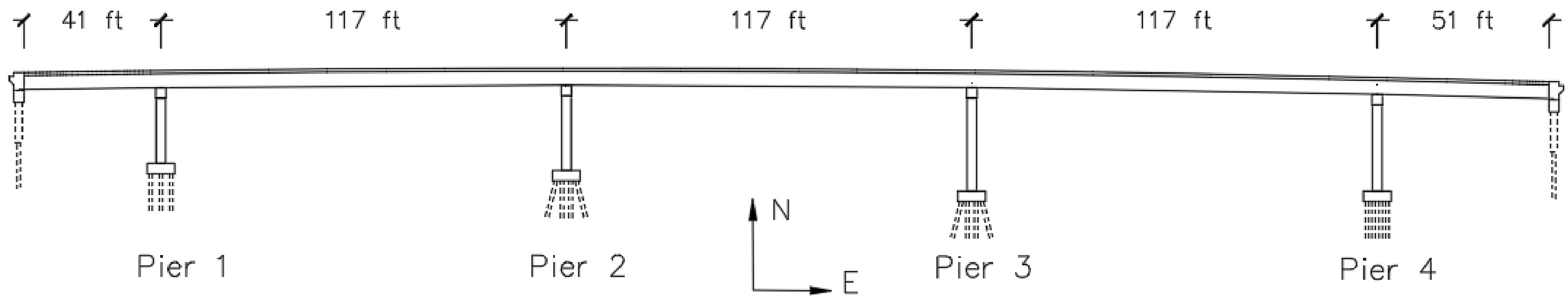

a) Side view

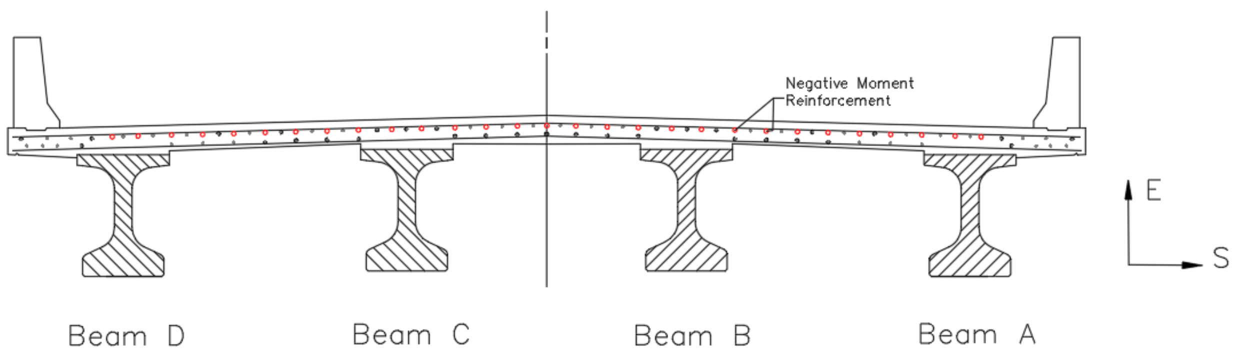

b) Cross-section view

Figure 3. E-57 over I-35 bridge drawings

3.2 Live Load Application and Instrumentation Plan

Three live load tests were conducted throughout the project duration: June 2018, June 2019, and June 2020. To aid in the interpretation of the data, the research team used controlled live load testing where a known load crosses the bridge at predetermined locations. By repeating this test every 12 months throughout the entire project, the data can be analyzed such that changes in behavior can be identified. During each live load test, a three-axle truck (with wheel spacings depicted in Figure 4) with a total weight of 27,400 lb, was driven across the bridge at a crawl speed (approximately 5 mph) to induce a pseudo-static load on the bridge.

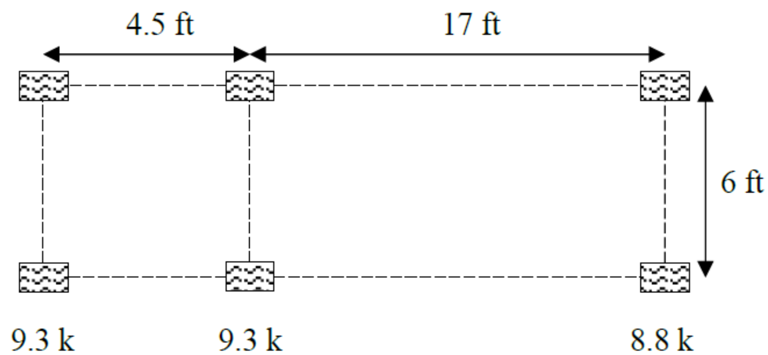

Figure 4. Truck information

Six load cases (LCs), as shown in Figure 5-b, with varying transverse locations of the vehicle were utilized.

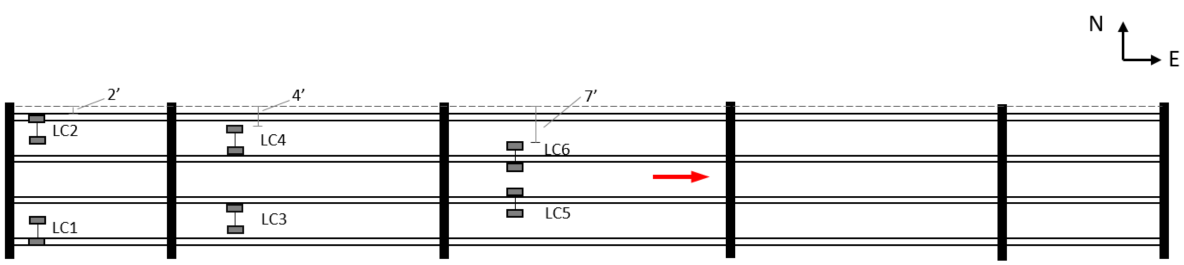

a) Load case position

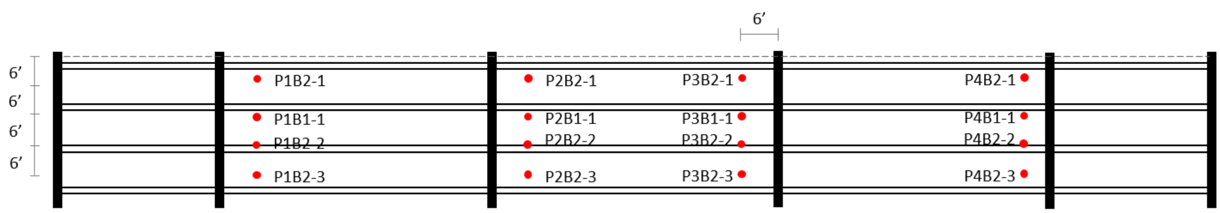

b) Deck embedded foil strain gauge

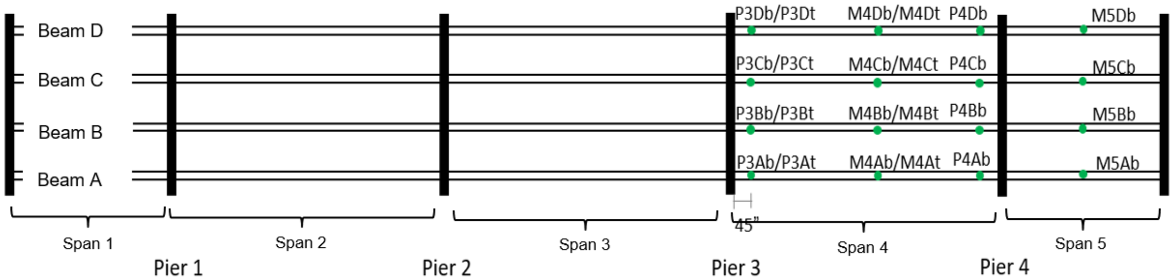

c) BDI Strain gauge

Figure 5. Load and instrumentation plan (plan view)

The same six LCs were used in each load test. In LC1, the truck was driven with the driver's wheel centerline offset by 2 ft from the south curb. In LC3, the truck was driven with the driver's wheel centerline offset from the south curb by 4 ft. In LC5, the truck was driven with the wheel offset from the curb by 7 ft.

Each-even numbered case was similar to its odd partner, but symmetric across the bridge's center line as shown. During testing, the data were marked every 10 ft of truck travel distance to allow the time collected by the strain gauges to be converted to a truck position along the length of the bridge.

During the tests, the strain data from 16 embedded strain gauges and 24 externally mounted strain gauges were collected to monitor the bridge behavior and identify differences in performance with the various reinforcing details. This data collecting system was configured so that the data could be used to study and report on the condition and behavior of the E-57 bridge.

The instrumentation work started during the bridge construction and prior to the placement of the deck concrete. The foil strain gauges were installed into four sections near the piers and about 6 ft away from the center of the pier diaphragm with four gauges in each section (see Figure 5-b). The label of each gauge was designed in such a way that P# designates the pier number, b2 designates the b2 bar, b1 denotes the conventional deck reinforcement b1 bar, and -# denotes the gauge number in each section. An image of an embedded gauge prior to the concrete deck pour is included later in Figure 7a.

Before each live load test, BDI strain gauges were attached on the exterior surface of the pre-stressed girder at four cross-sectional locations in the eastern two spans (see Figure 5-c). At Pier 3 and the middle of the fourth span sections, the gauges were installed on both the top and bottom of the flange, while in the section near Pier 4 and the middle of the fifth span, gauges were installed only on the bottom flange. The labels on the BDI strain gauge were designated such that P3 and P4 denote the sections near Pier 3 and Pier 4, respectively, M4 and M5 denote the middle span of the fourth span and fifth span, respectively, the third alphabetic (capital) letter denotes the beam number, and the fourth alphabetic (lowercase) letter denotes the locations with t for top of girder and b for bottom of girder. Figure 6 shows the gauge locations in a cross-section view.

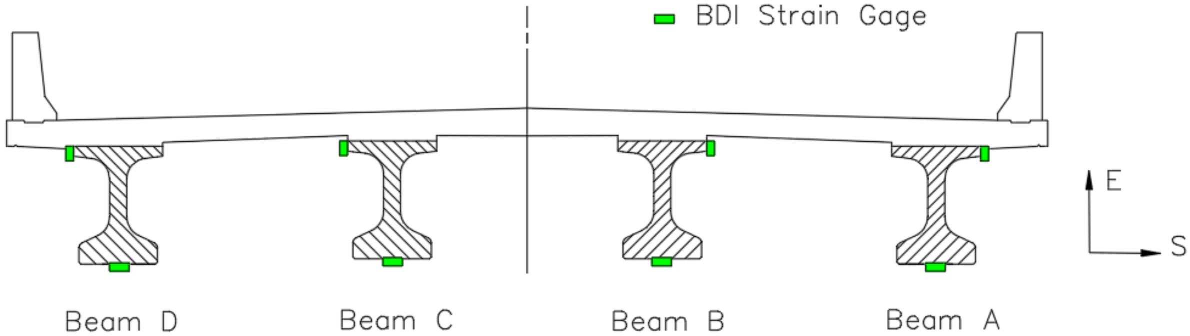

Figure 6. BDI gauges instrumentation (cross-section view)

Figure 7 shows the field instrumentation images.

a) Embedded strain gauge

b) BDI strain gauge

Figure 7. Field instrumentation

3.3 Live Load Test Results

Although in each test, six LCs with different transverse truck locations were performed, only the results from LC2 when the truck was driven at a distance of 2 ft off the north curb are presented in this report for brevity. This is because the bridge is not skewed, and the test results indicated good overall symmetric behavior of the bridge.

The data measured by the embedded foil strain gauges and attached BDI strain gauges during each test in 2018, 2019, and 2020 are presented through Section 3.3.1, 3.3.2, and 3.3.3, respectively. A short discussion of the comparison of the data from different years is presented in Section 3.3.4.

3.3.1 2018 Test

The 2018 test consisted of two separate load tests. The first test was conducted on June 20. The results from the first test indicated that only the BDI gauges recorded valid strain data, and data from foil strain gauges showed significant noise, likely induced by the generator. The test was then repeated on July 13. During the second test in 2018, only foil strain gauges were used to collect the data. Hence, the data from the BDI and embedded gauges were collected from different tests in 2018. This had no effect on the data or the results that were seen.

Figure 8 shows the data measured by the gauges embedded in the deck.

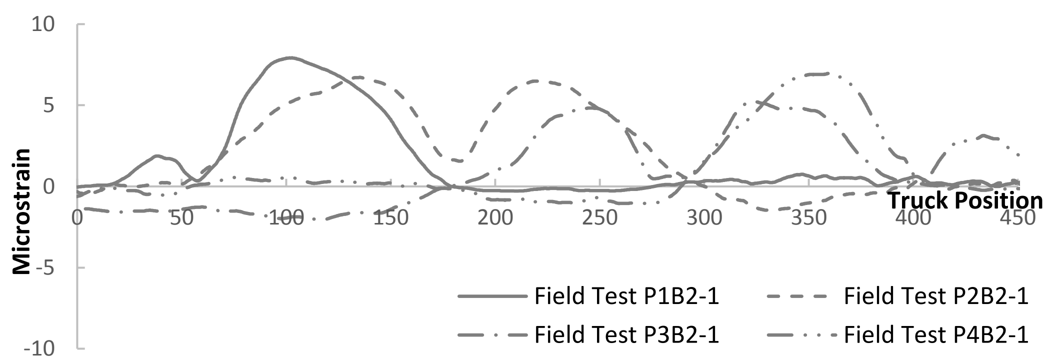

a) Deck rebar strain-1

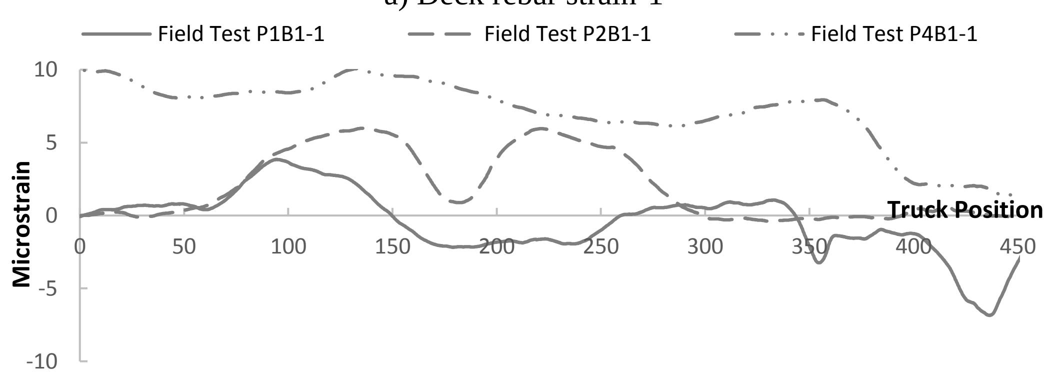

b) Deck rebar strain-2

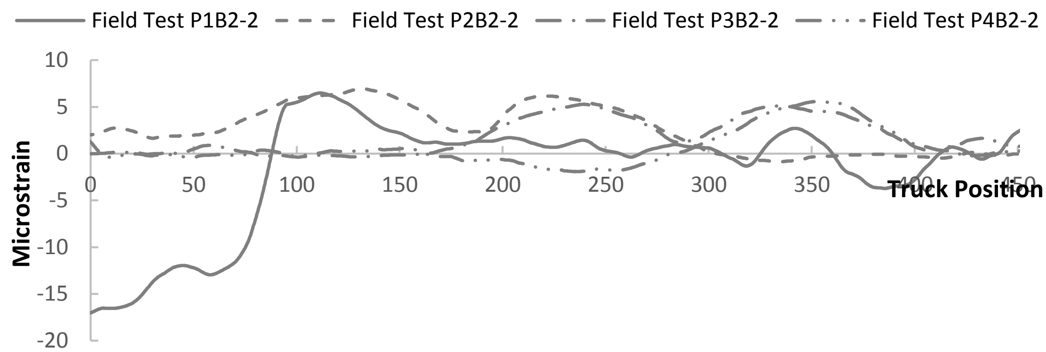

c) Deck rebar strain-3

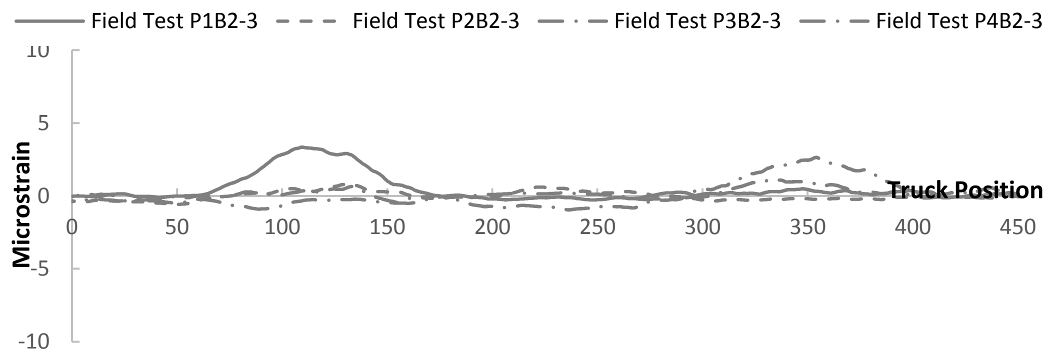

d) Deck rebar strain-4

Figure 8. 2018 deck strain data (LC2)

Figure 9 and Figure 10 show the strain measured from external strain gauges on the girder.

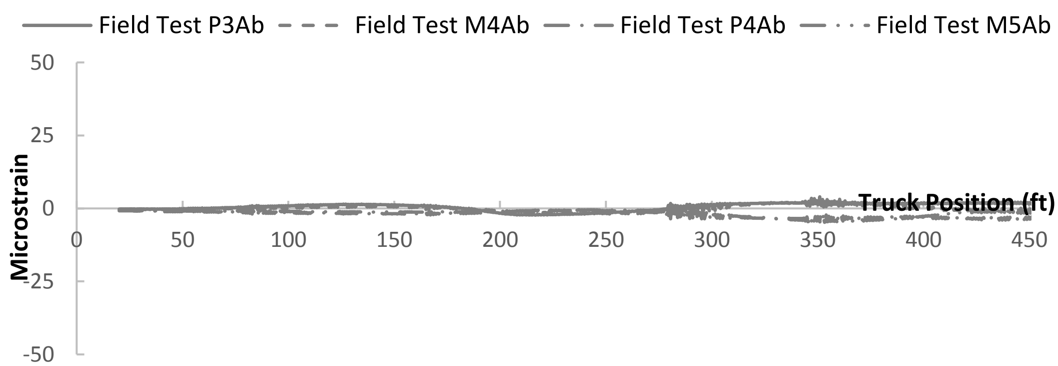

a) Strain obtained from Beam A

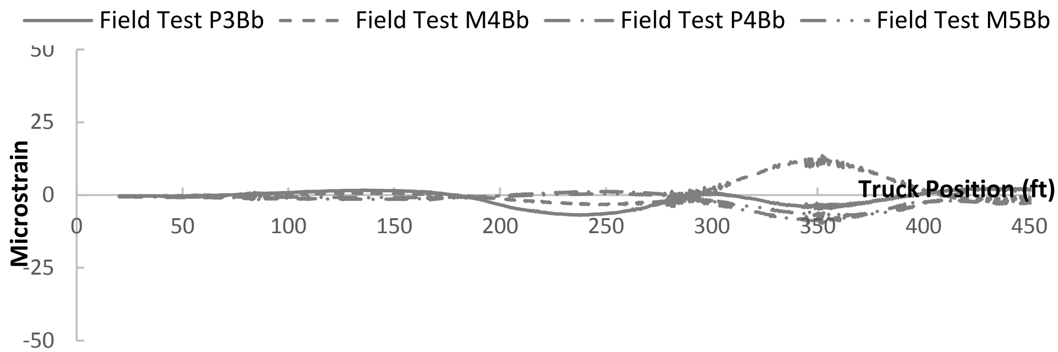

b) Strain obtained from Beam B

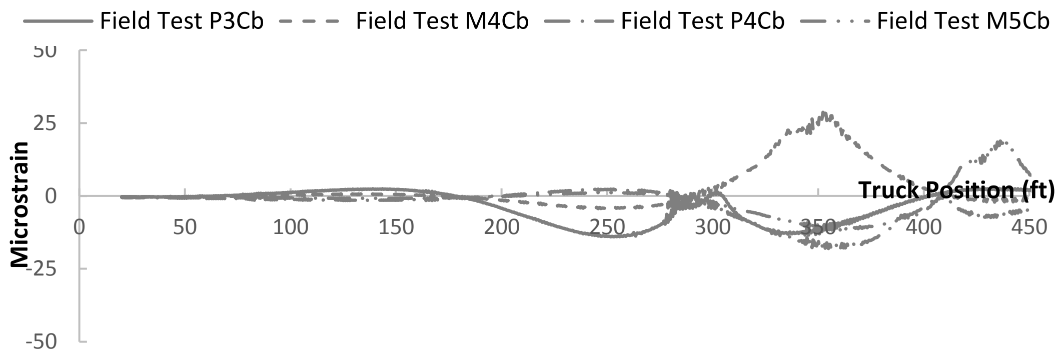

c) Strain obtained from Beam C

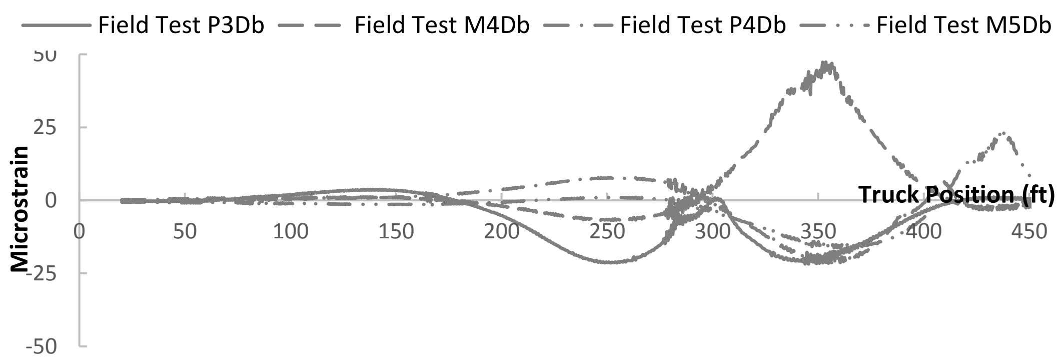

d) Strain obtained from Beam D

Figure 9. 2018 strain data at bottom flange (LC2)

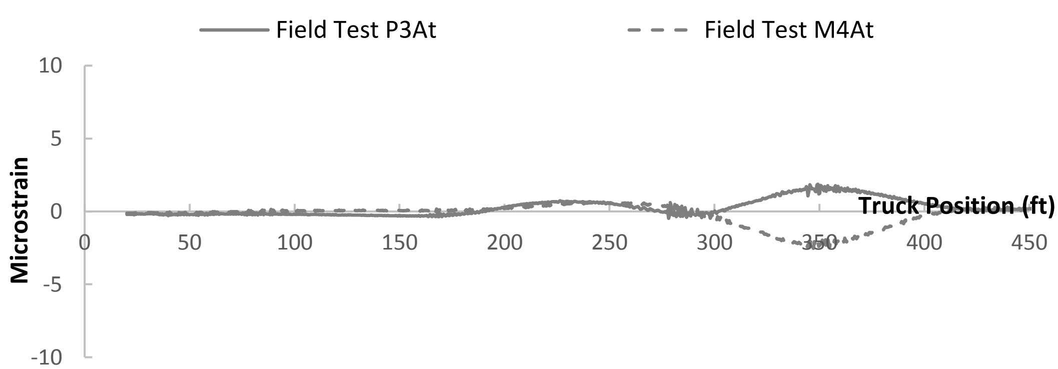

a) Strain obtained from Beam A

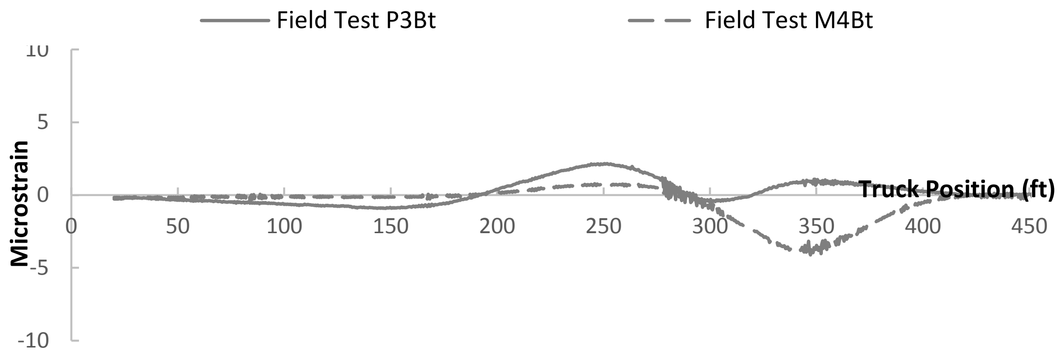

b) Strain obtained from Beam B

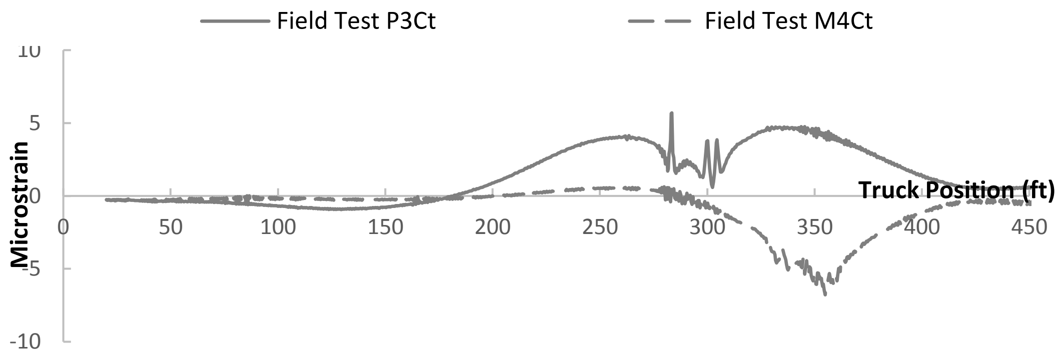

c) Strain obtained from Beam C

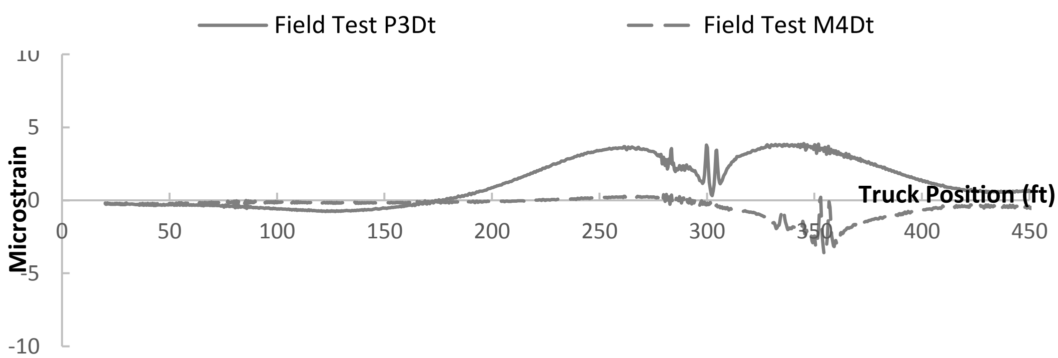

d) Strain obtained from Beam D

Figure 10. 2018 strain data at top flange (LC2)

3.3.2 2019 Test

The 2019 load test was conducted on June 10. For all six load cases, the truck was driven from the east end to the west end. To compare with the data from 2018, the data were plotted reversely, and started from the west end in Figure 11 for the embedded strain gauges and Figure 12 and Figure 13 for the embedded strain gauges. This is the cause for slight differences regarding the location of the peak strain in some figures.

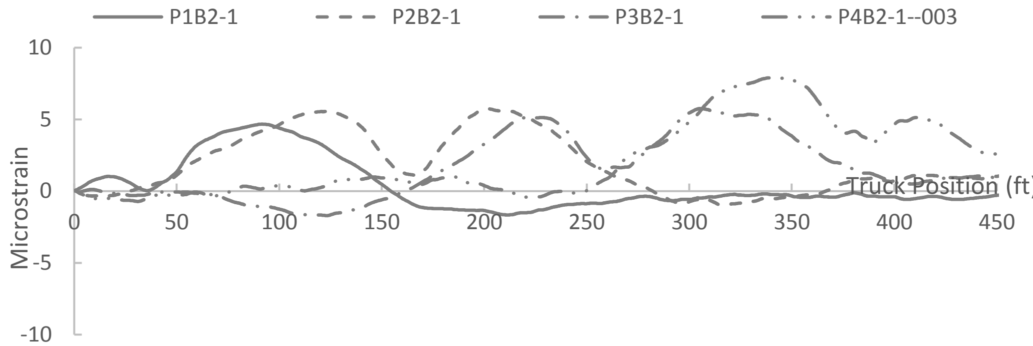

a) Deck rebar strain-1

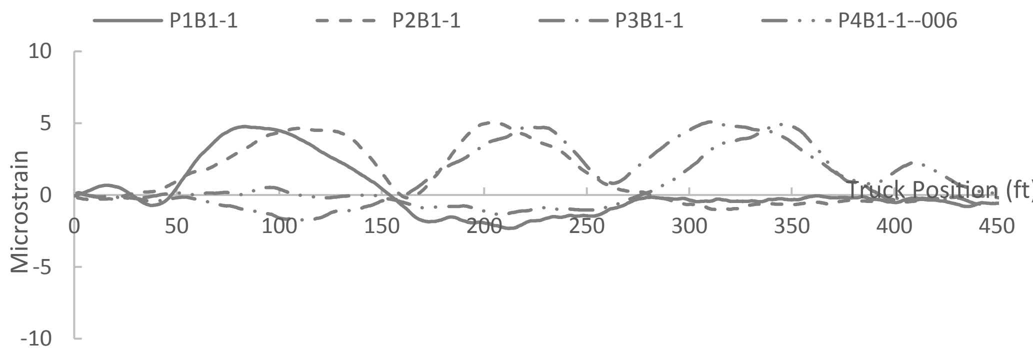

b) Deck rebar strain-2

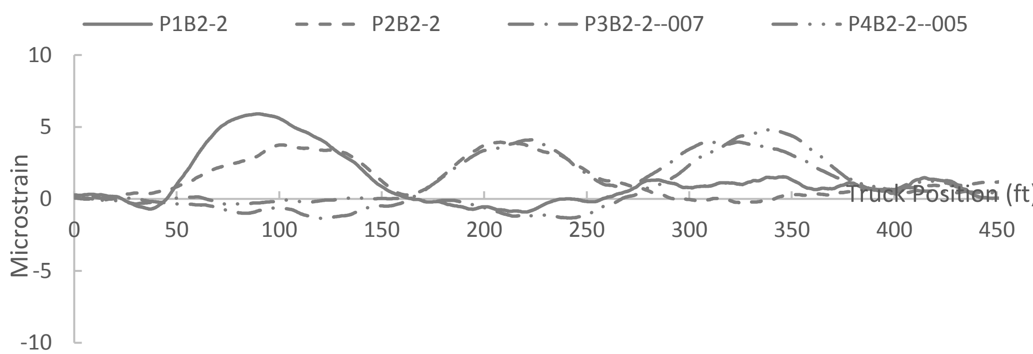

c) Deck rebar strain-3

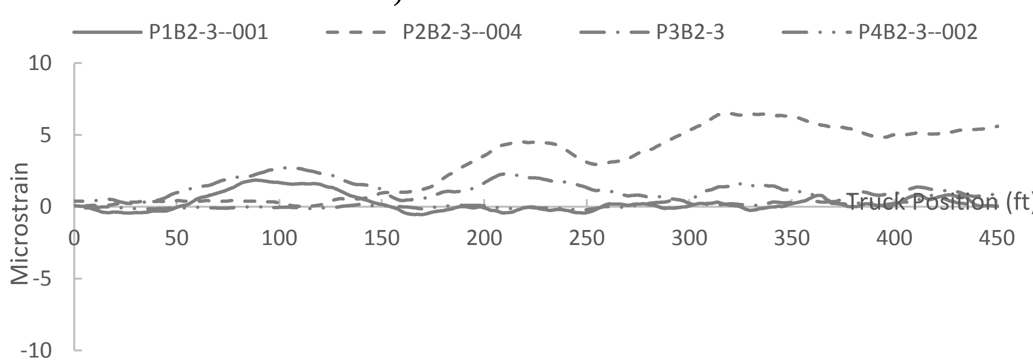

d) Deck rebar strain-4

Figure 11. 2019 deck strain data (LC2)

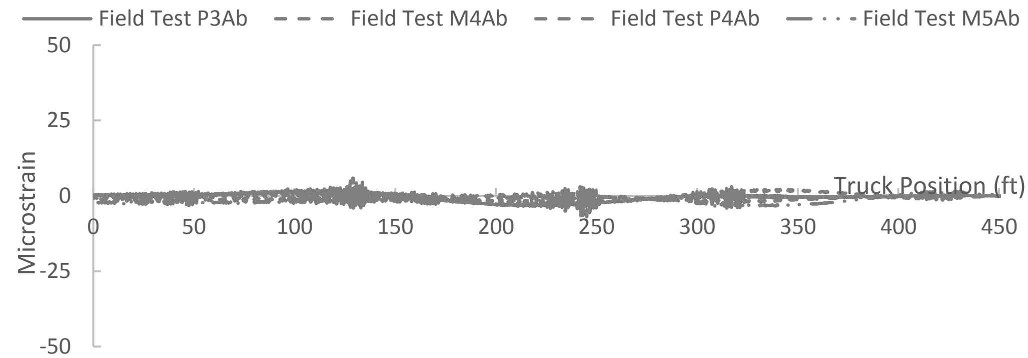

a) Strain obtained from Beam A

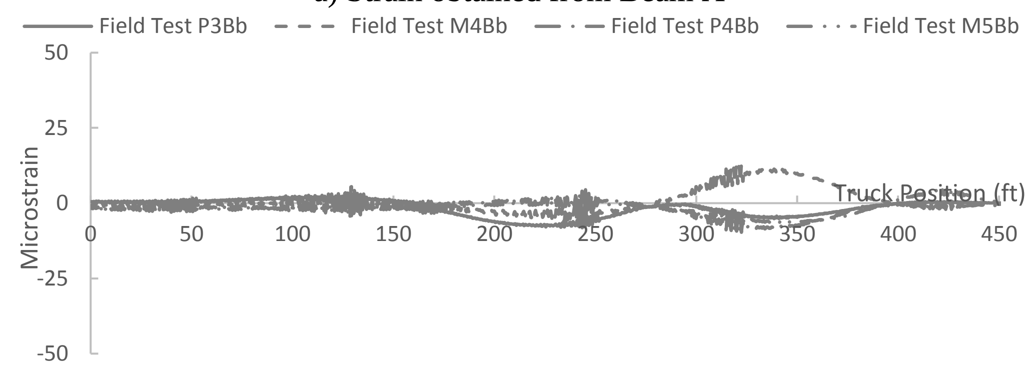

b) Strain obtained from Beam B

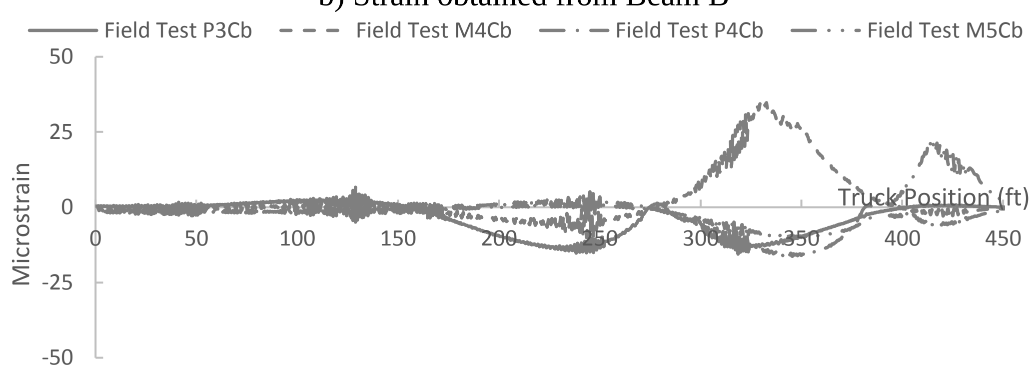

c) Strain obtained from Beam C

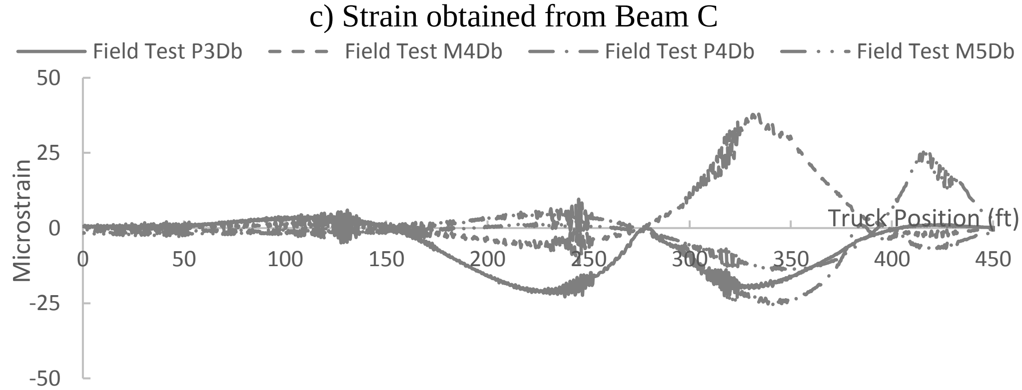

d) Strain obtained from Beam D

Figure 12. 2019 BDI strain data at bottom flange (LC2)

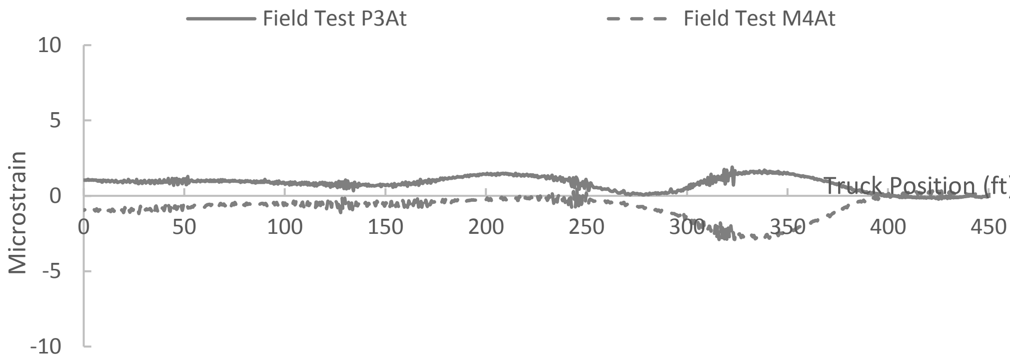

a) Strain obtained from Beam A

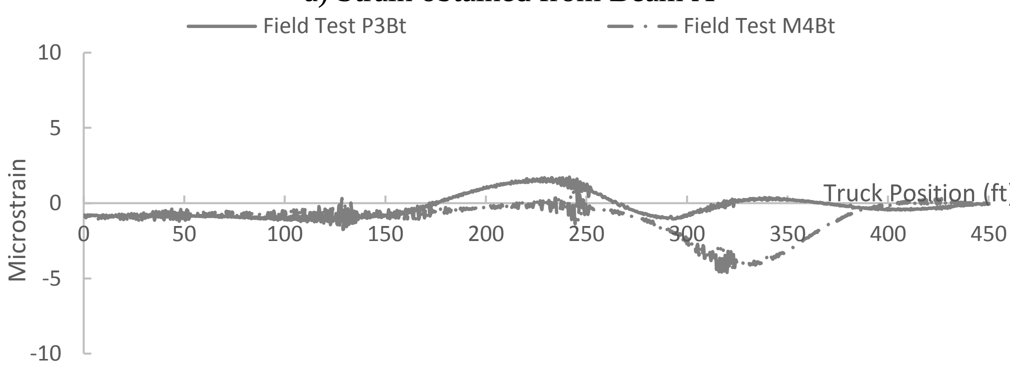

b) Strain obtained from Beam B

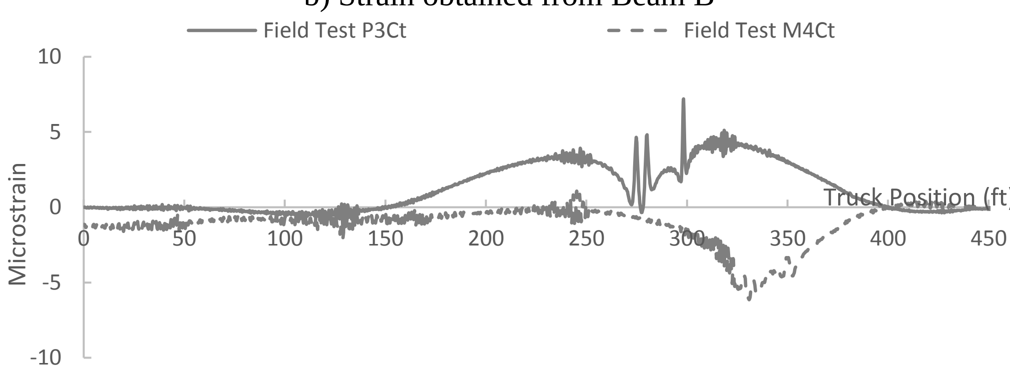

c) Strain obtained from Beam C

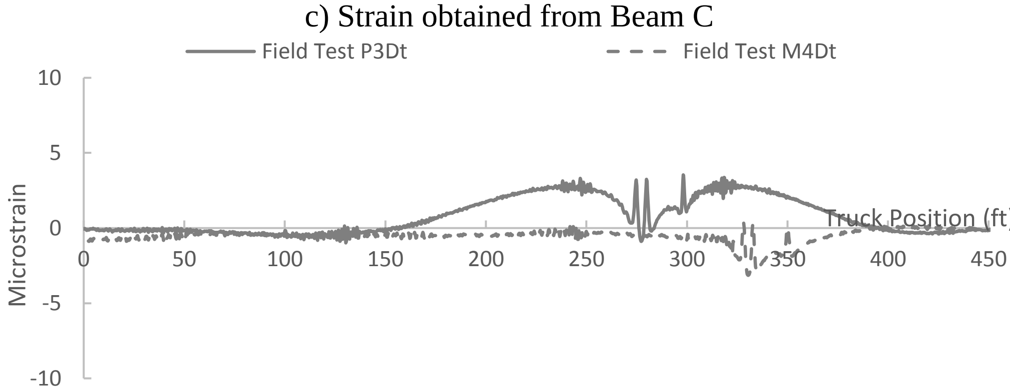

d) Strain obtained from Beam D

Figure 13. 2019 BDI strain data at top flange (LC2)

3.3.3 2020 Test

The 2020 load test was conducted on June 23, mirroring the protocol used in 2019. For all six load cases, the truck was driven from the east end to the west end. The data are plotted in Figure 14 through Figure 16.

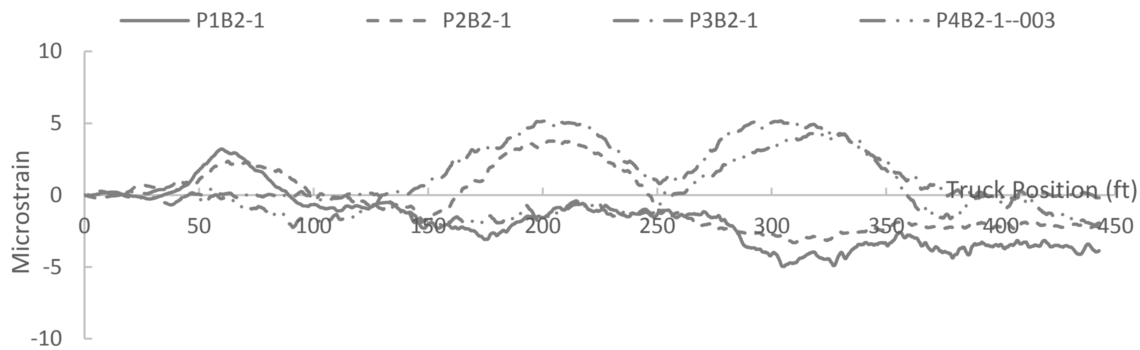

a) Deck rebar strain-1

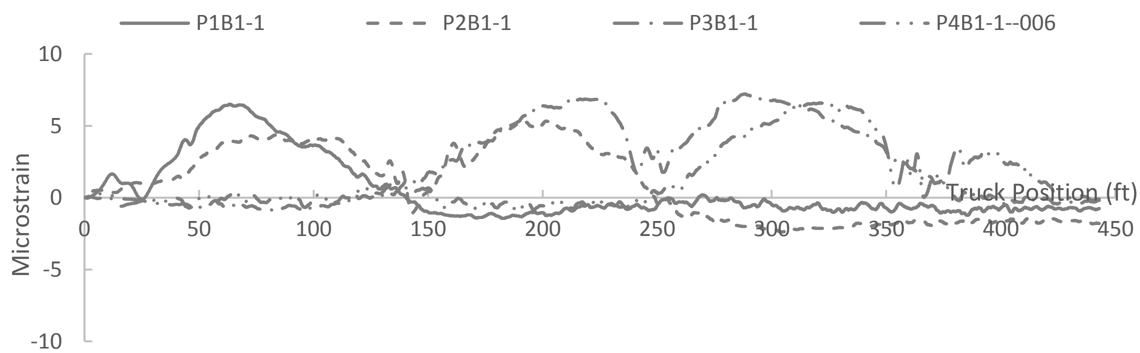

b) Deck rebar strain-2

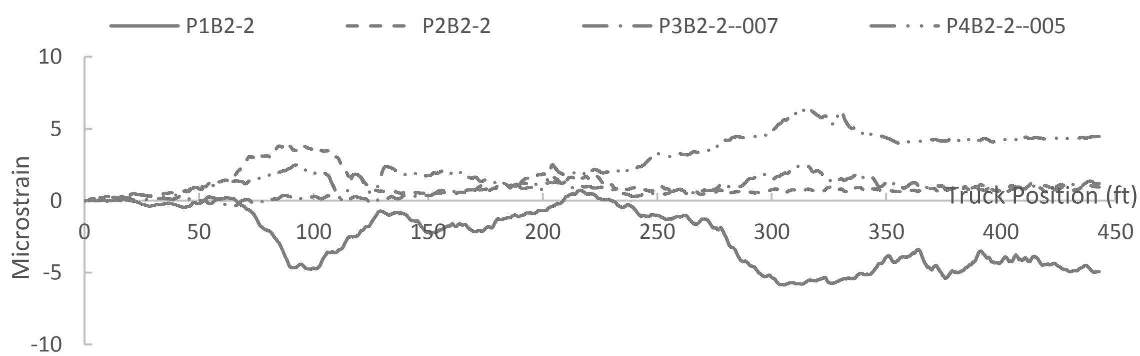

c) Deck rebar strain-3

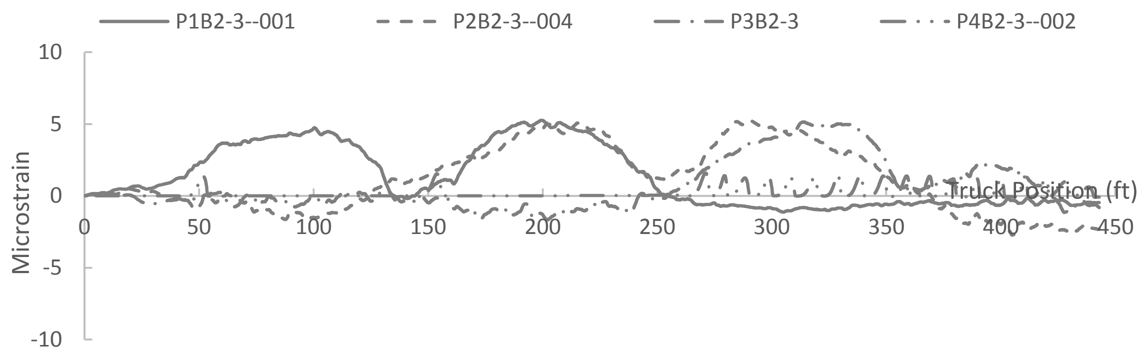

d) Deck rebar strain-4

Figure 14. 2020 deck strain data (LC2)

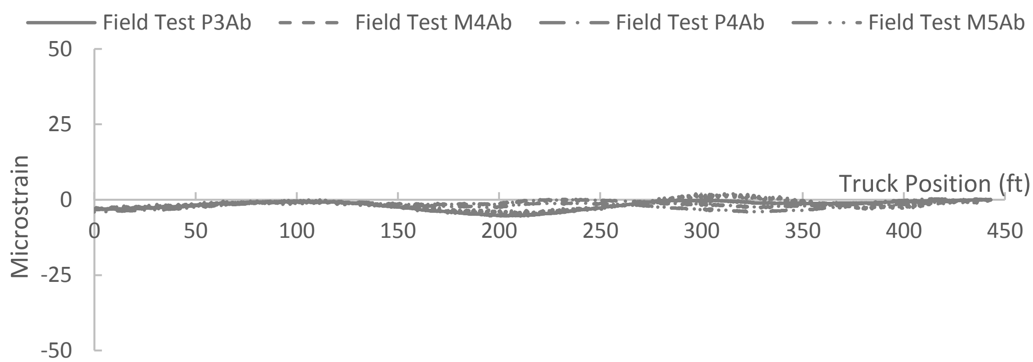

a) Strain obtained from Beam A

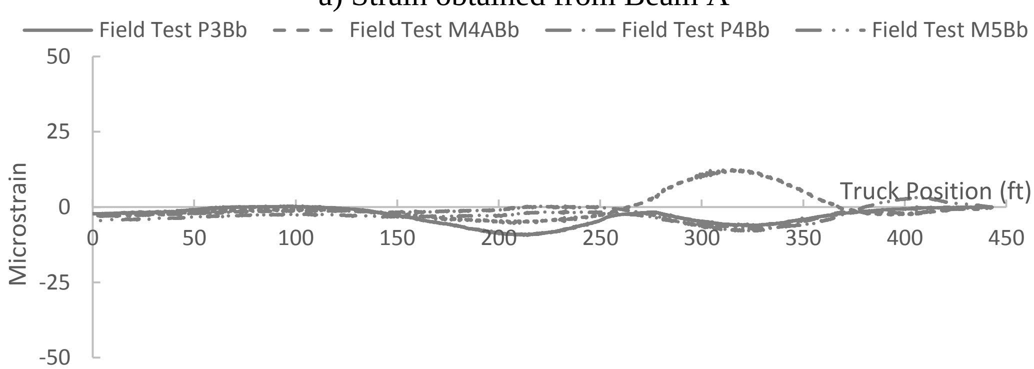

b) Strain obtained from Beam B

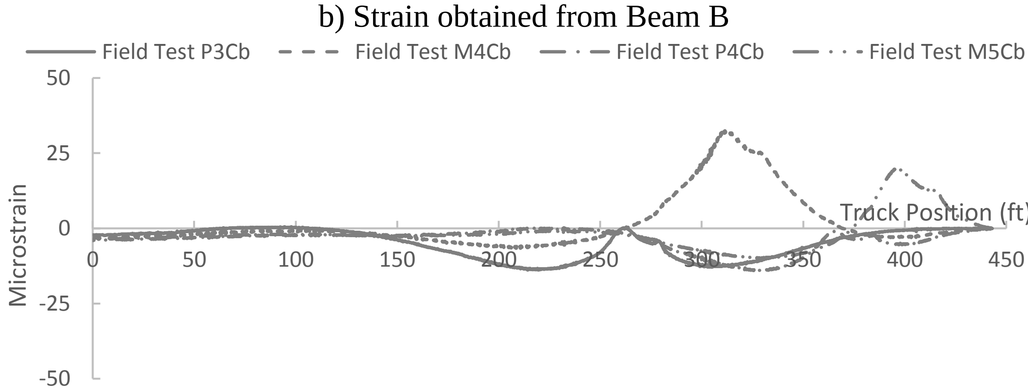

c) Strain obtained from Beam C

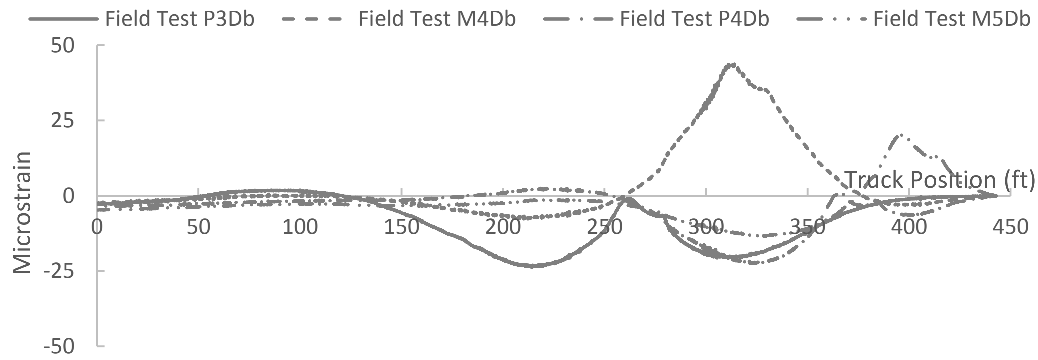

d) Strain obtained from Beam D

Figure 15. 2020 strain data at bottom flange (LC2)

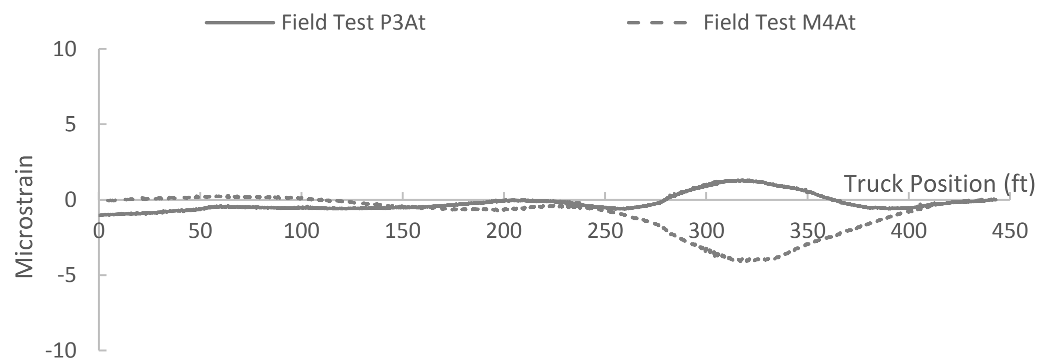

a) Strain obtained from Beam A

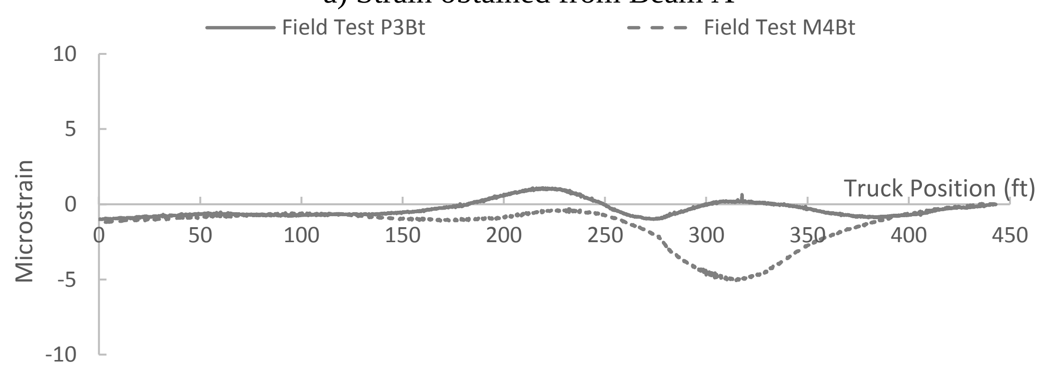

b) Strain obtained from Beam B

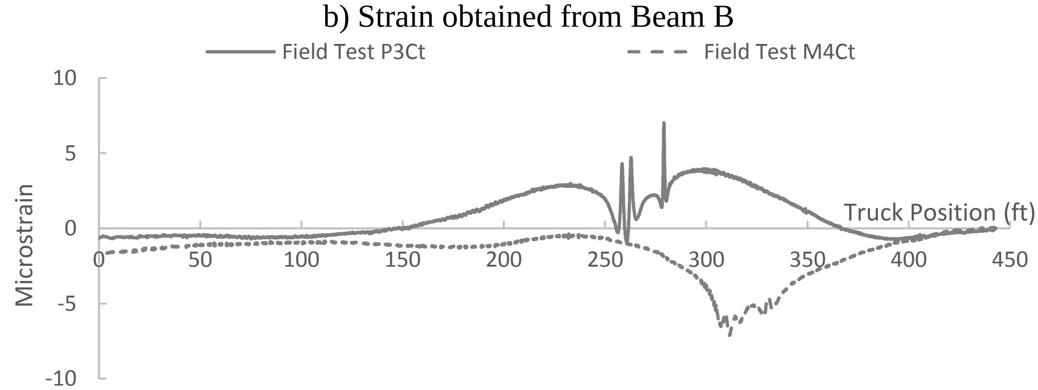

c) Strain obtained from Beam C

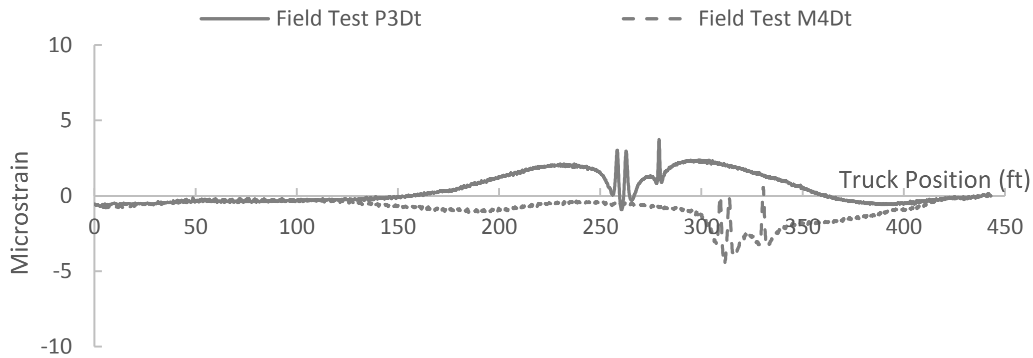

d) Strain obtained from Beam D

Figure 16. 2020 strain data at top flange (LC2)

3.3.4 Field Test Results Discussion

The data from all the strain gauges indicated that the strain on both the b1 and b2 bars are in very minimal tension (less than 10 microstrain). It can be concluded from the field test data that the negative moment occurs when the bridge was subjected to the live load; however, the reinforcement (b1/b2 bars) showed a minimum effect with respect to resisting the negative moment before deck crack formation.

Figure 17 compares the strain data over the years in gauge M4Db and P1B2-1.

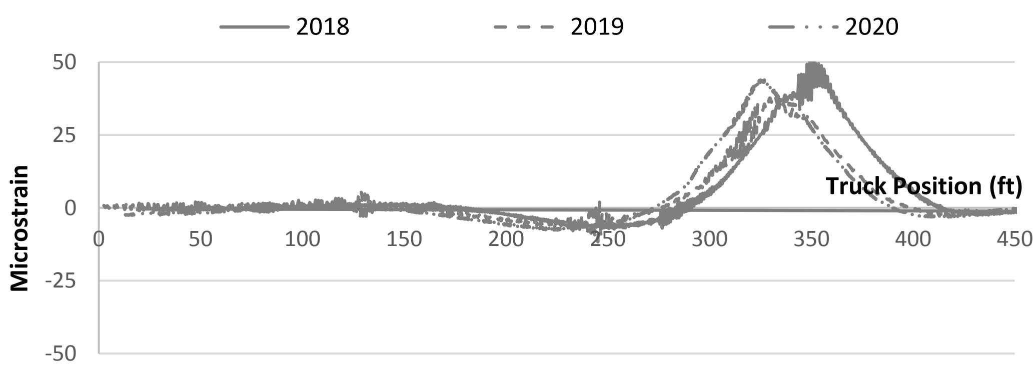

a) M4Db

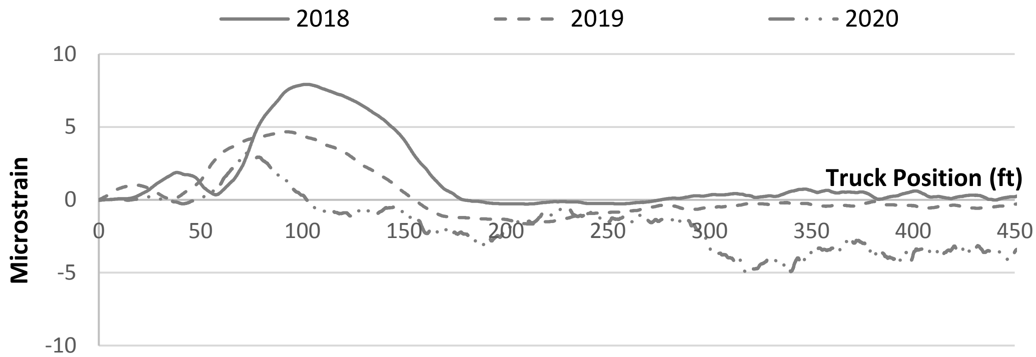

b) P1B2-1

Figure 17. Data comparison over the years

Both the deck strain and girder bottom strain indicated that the measured strain decreased slightly each year. This is likely due to the increase of the concrete strength, although the magnitudes of the strains are very small.

Comparing the data in 2018 to that from the 2019 and 2020 tests, no significant strain increase was found. This indicates that no cracks could be detected in the vicinity of the instrumentation. These results show good agreement with the crack inspection results, such that no cracks could be found from 2018 to 2020.

3.4 Field Inspection

In addition to the controlled load tests, the research team conducted bridge inspections (primarily focused on the deck) every six months for the duration of the project. The objective of the bridge inspections was to document the cracks (if any) in the deck and track them during future inspections. However, by the final inspection in December 2020, no cracks were visually observed on the top surface of deck near the piers. Figure 18 shows the bridge top surface.

Figure 18. Bridge deck top surface

The absence of bridge deck cracks shows an agreement with the strain data from the rebar in the deck over the piers, as they were consistently small (less than 10 microstrain) from 2018 to 2020.

CHAPTER 4. ANALYTICAL STUDY

The objective of the analytical study was to investigate the performance of b2 rebars subjected to the negative moment induced by both live loads and secondary moments. First, the researchers established a full-scale bridge FEM utilizing the commercially available finite element analysis software ANSYS and validated the model against the field test collected data. They investigated the effectiveness of different amounts of b2 bars at resisting the negative moment induced by live loads on a full-scale basis. Secondly, they calculated the negative moment induced by the secondary moment over each pier using mRESTRAINT. In the third step, a small-scale FEM was developed using the same modeling approach as that used on the full-scale model and loaded with the negative moment estimated using mRESTRAINT. The performance of different amounts of b2 bars was then investigated on the small-scale FEM.

4.1 Full-Scale Model

4.1.1 Model Development

The goal of developing the full-scale FEM was to analytically study the ability of the reinforcement to resist the negative moment induced by live loads and to provide modeling guidance for development of the small-scale model. A full-scale model with discrete b2 bars was initially developed and validated against the field test results. Another model without b2 bars was then developed using the same modeling approach. The effect of different amounts of b2 bars was evaluated by comparing the stress distribution from both models.

The full-scale model was developed for the superstructure of the bridge including the deck, prestressed concrete girders, abutments, pier diaphragms, and barrier. The piles under the abutments and the bearings between the prestressed concrete beam and pier cap were simplified by using the simple support condition. Figure 19 shows the first and second span of the full-scale model.

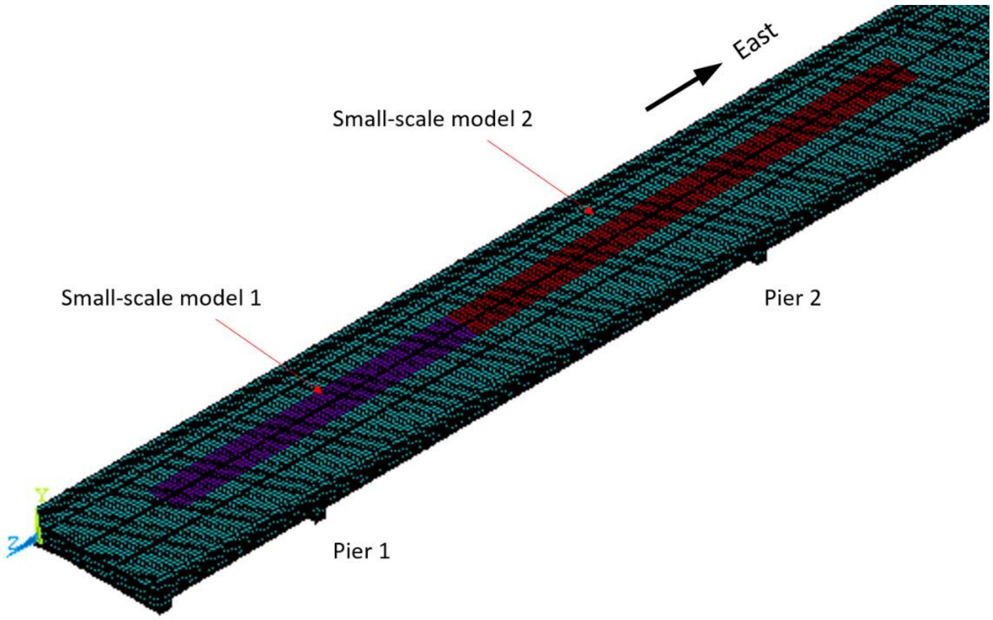

Figure 19. Full-scale bridge model

All of the concrete components were modeled using 3D Solid65 elements and the b2 bars were modeled by using discrete Beam183 elements. A perfect bond between the concrete and the reinforcement was assumed by merging the nodes on the solid elements and beam elements.

Given there was no significant cracking found on the deck over the piers, an elastic model was developed to predict the stress distribution in the superstructure. Table 1 lists the compressive strength (f_c') and Young's Modulus (E) of each concrete component.

Table 1. Material properties

	41 ft pre-stressed concrete beam		51 ft pre-stressed concrete beam		117 ft pre-stressed concrete beam		Cast-in-place concrete (deck, abutment, pier diagram)	
	f_c'(ksi)	E (ksi)	f_c'(ksi)	E (ksi)	f_c' (ksi)	E (ksi)	f_c' (ksi)	E (ksi)
Design drawing	5	4,031	5	4,031	9	5,407	4	3,605
Material tests (28th day)	11.5	6,113	11.5	6,113	11.8	6,192	5.6	4,265

The bridge plans specified a compressive strength of 4 ksi for the deck, abutment, and pier diaphragm concrete, 5 ksi for prestressed concrete girders in the exterior spans, and 9 ksi for the girders in the interior spans. However, the material tests at 28 days indicated higher compressive strength values: 5.6 ksi for the deck, abutment, and pier diaphragm concrete, 11.5 ksi for the prestressed concrete girders in the exterior spans, and 11.8 ksi for the girders in the interior spans. The compressive strength obtained from the material tests were used to calculate Young's Modulus by using $57{,}000\sqrt{f_c'}$ (ACI 2011), resulting in 6,113 ksi and 6,192 ksi for the girders in the exterior and interior span, respectively, and 4,265 ksi for the other concrete components. The conventional transverse and longitudinal reinforcement in the top and bottom mat were smeared into the deck solid element by calculating an effective Young's Modulus (E_{eff}) in each direction using Equation 1 and assigning an orthotropic material behavior.

$$\boldsymbol{E_{eff}} = \frac{\boldsymbol{A_c E_c + A_s E_s}}{\boldsymbol{A_c + A_s}} \tag{1}$$

E_{eff} = effective linear elastic modulus of combined steel and concrete
A_c = area of concrete
A_s = area of steel
E_c = linear elastic modulus of concrete
E_s = linear elastic modulus of steel (29,000 ksi)

The Young's Modulus for the reinforcing steel was set as 29,000 ksi.

4.1.2 Model Validation

The model and the modeling approach were validated by the field data collected from the tests in 2018. Figure 20 compares the analytical results to the field strain data collected from the strain gauges embedded in the deck.

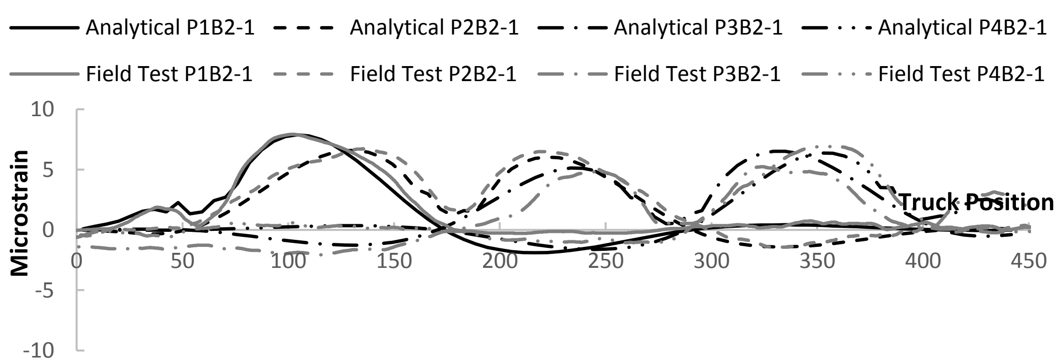

a) Deck rebar strain-1

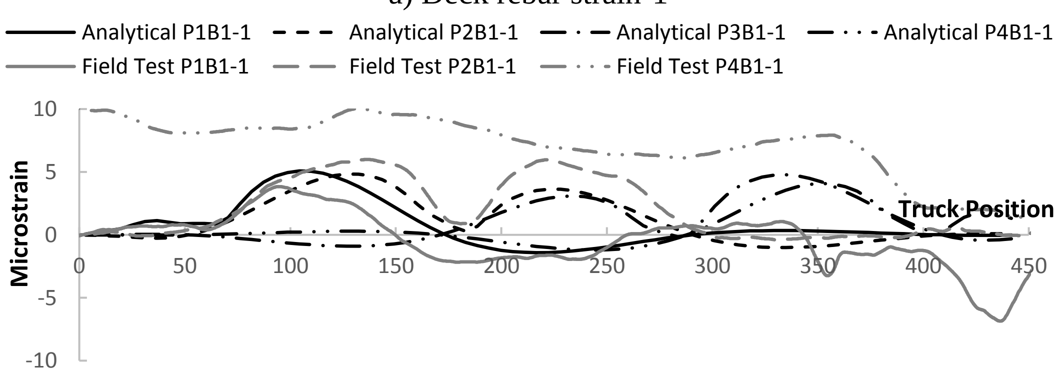

b) Deck rebar strain-2

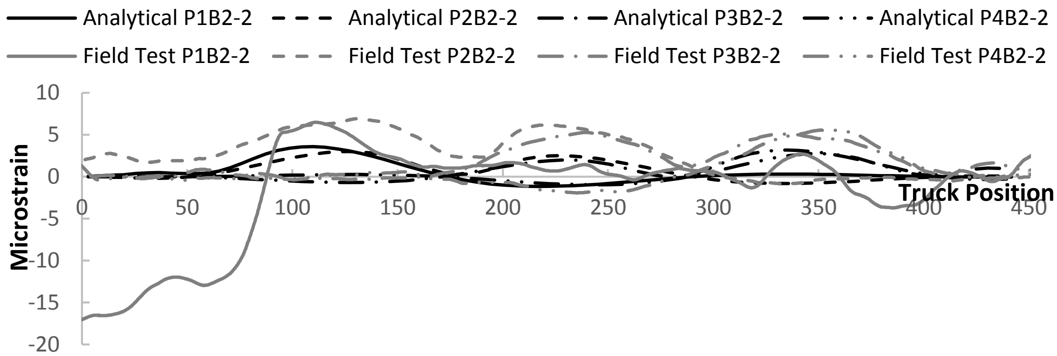

c) Deck rebar strain-3

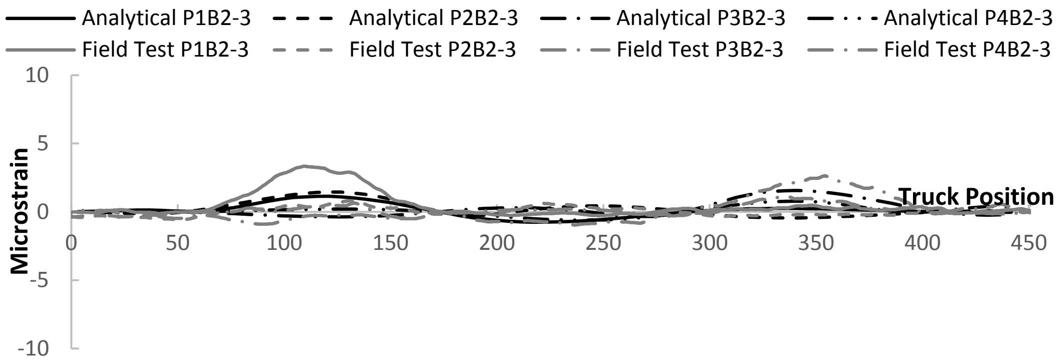

d) Deck rebar strain-4

Figure 20. Validation by deck strain data (LC2)

Figure 21 and Figure 22 compare the analytical results to the live load test results for the external gauges attached at the bottom flange and top flange, respectively.

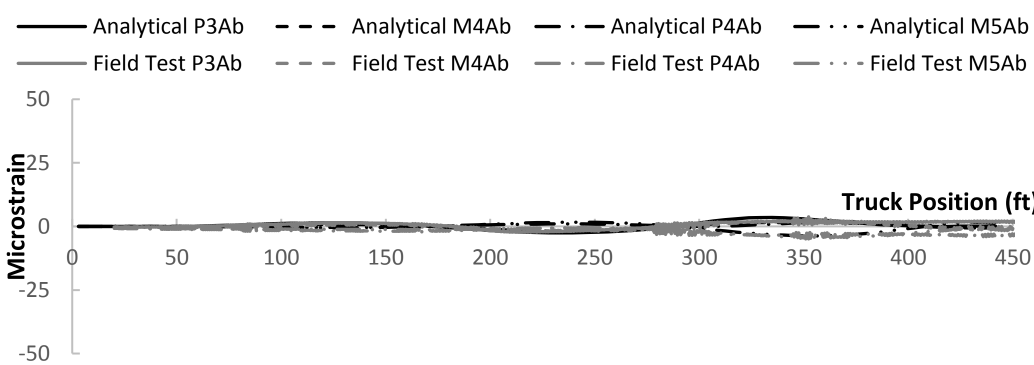

a) Strain obtained from Beam A

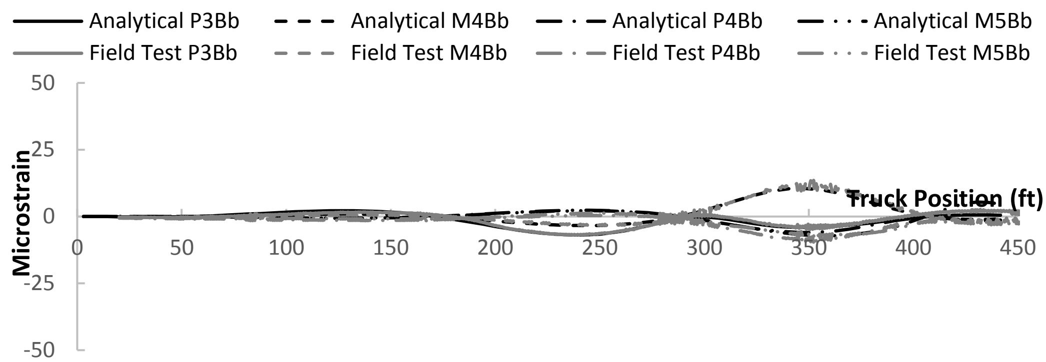

b) Strain obtained from Beam B

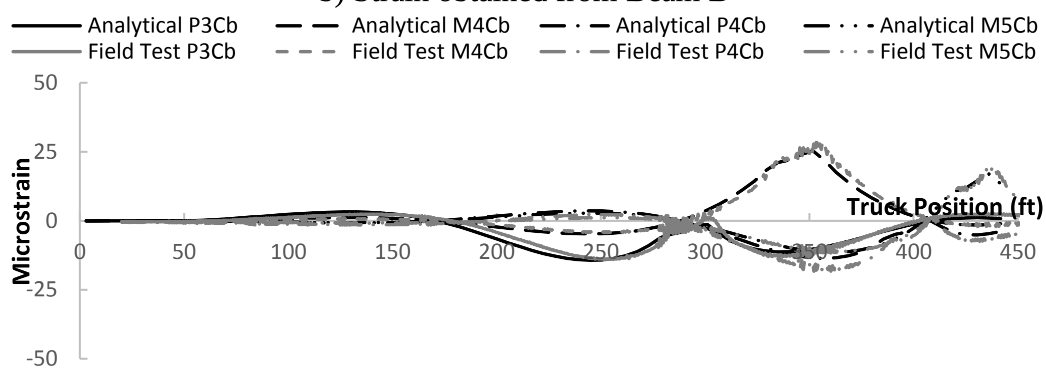

c) Strain obtained from Beam C

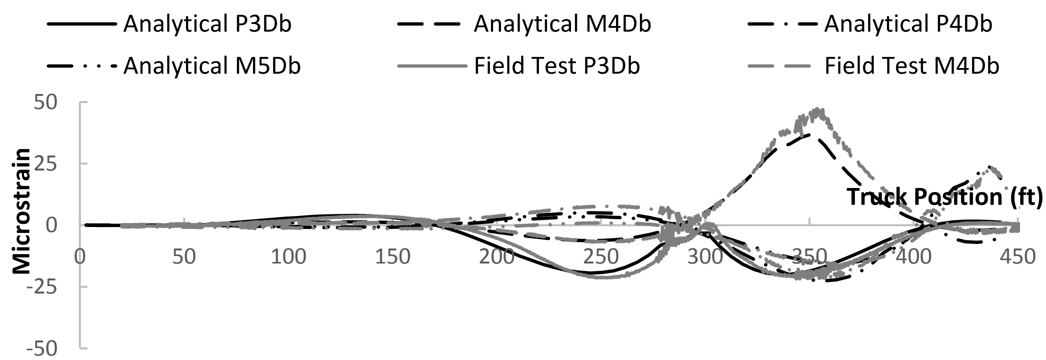

d) Strain obtained from Beam D

Figure 21. Validation by BDI strain data at bottom flange (LC2)

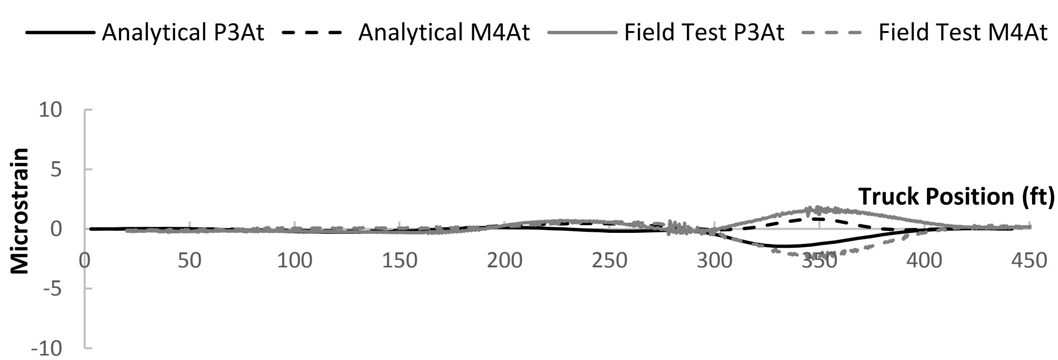

a) Strain obtained from Beam A

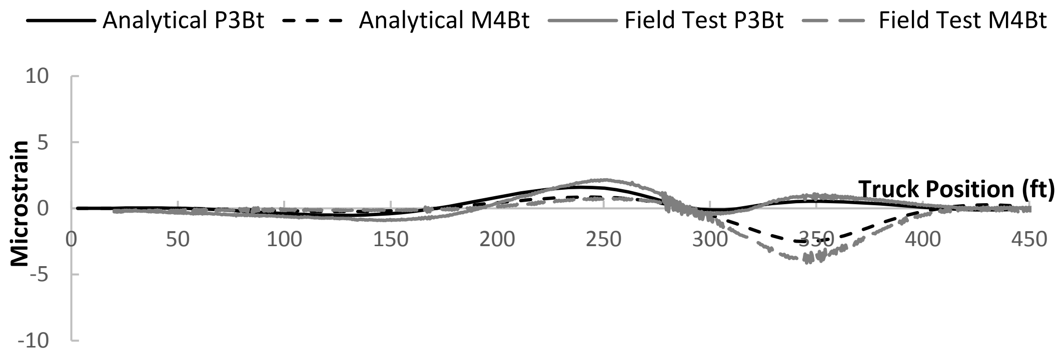

b) Strain obtained from Beam B

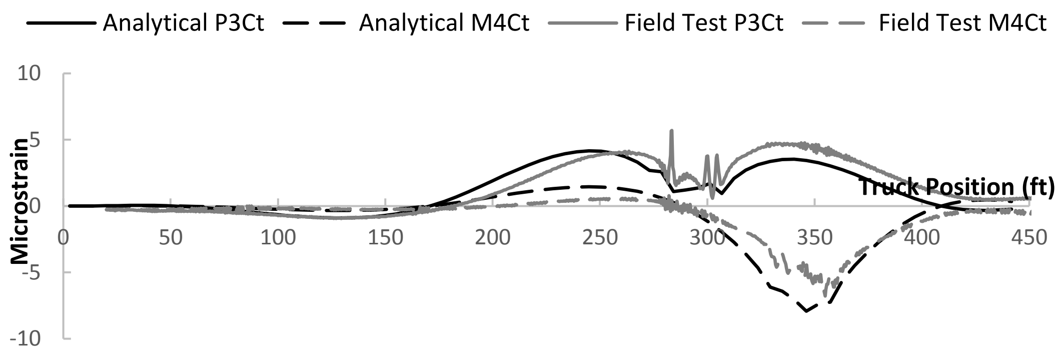

c) Strain obtained from Beam C

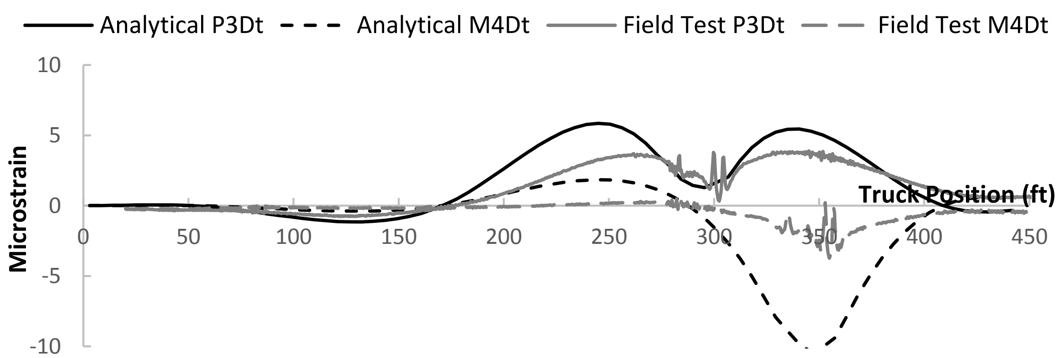

d) Strain obtained from Beam D

Figure 22. Validation by BDI strain data at top flange (LC2)

The gauge locations were previously shown in Figure 5. Comparing the strains collected from Pier 1 and 4 to the strains collected from Pier 2 and 3, no significant difference can be observed from the data, although the negative moment reinforcement over each pier was designed with different purposes and contained significantly different amounts of reinforcement. In general, the analytical results showed good agreement with the field test results. As such, no further calibration was performed on the FEM.

4.1.3 Effect of B2 Bars

To investigate the efficiency of the longitudinal reinforcement at resisting the negative moment, another FEM was developed using the same modeling approach and subjected to the same loading, except the longitudinal b2 bars over each pier were removed. Figure 23 and Figure 24 compare the longitudinal stress-induced-strain on the top surface of the deck over each pier subject to the truck load from LC2.

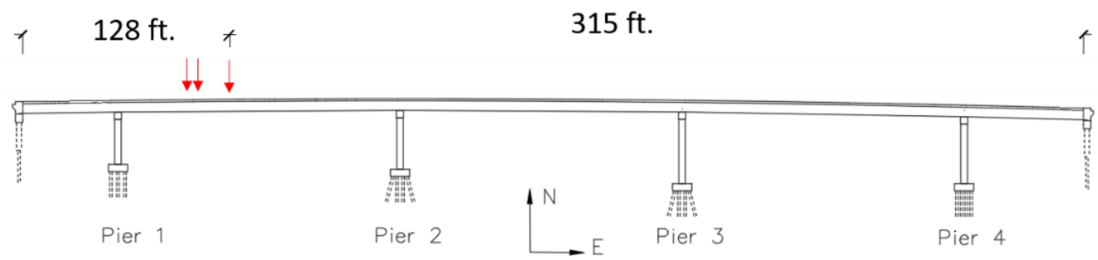

a) Truck position

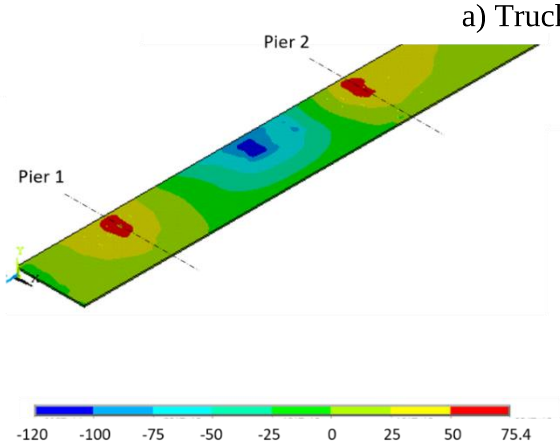

b) With b2 bar (με)

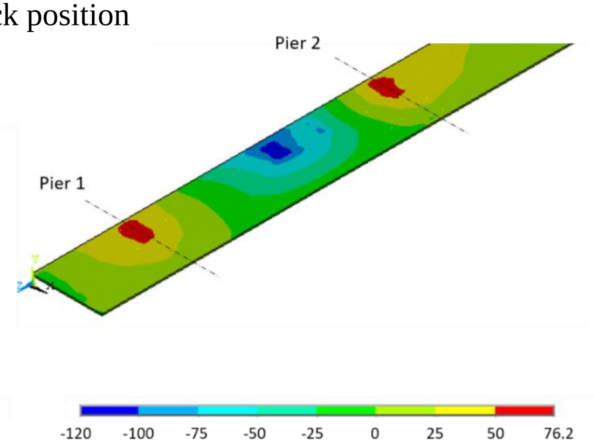

c) Without b2 bar (με)

Figure 23. Deck top stress-induced-strain over Pier 1 and 2

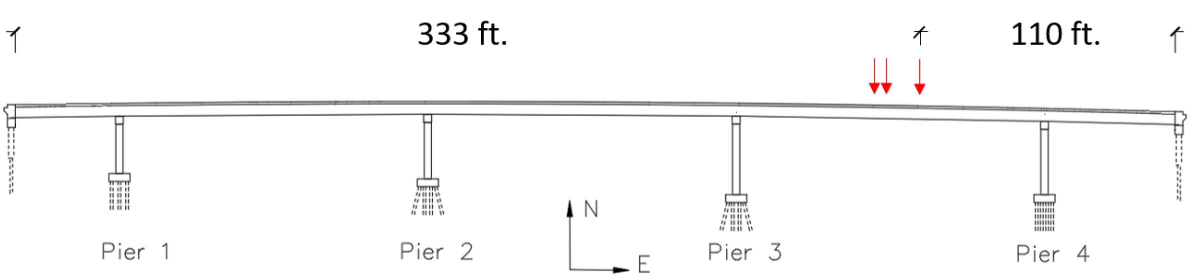

a) Truck position

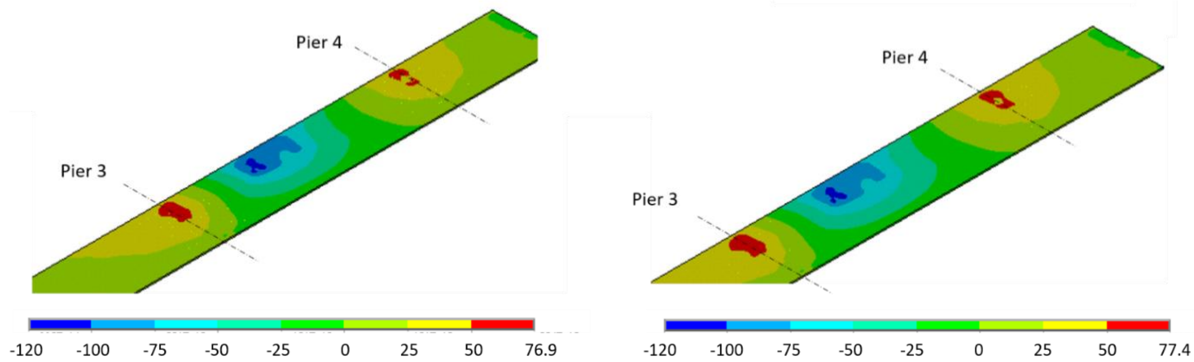

b) With b2 bar (με) c) Without b2 bar (με)

Figure 24. Deck top stress-induced-strain over Pier 3 and 4

Figure 23-a and Figure 24-a show the longitudinal truck position, which generates the maximum negative moment over the piers of interest. It was found that there was no significant difference in the strain distribution in the deck between the FEMs with and without the b2 bar, although the maximum strains in the model without b2 reinforcing steel were very slightly increased. It should be noted that the maximum strain (75.4 to 77.4 microstrain) on the top of the bridge deck over the piers is less than the concrete cracking strain of 132 microstrain as calculated by $7.5\sqrt{f_c'}/57{,}000\sqrt{f_c'}$ (ACI 2011).

Comparing the deck top strain with the strain (less than 10 microstrain) measured from the b2 bars, it can be concluded that a significant strain gradient developed through the deck depth in the area of the negative moment region. The analytical results show consistency with the field test results in that the b2 reinforcing steel contributed minimally to resisting the negative moment induced by the live load before any deck cracks formed.

4.2 Calculation of Secondary Moment

The secondary moment was calculated utilizing the spreadsheet-based program, mRESTRAINT. The deck and girder long-term shrinkage was calculated utilizing Equation 2 (AASHTO 2012, Eq. 5.4.2.3.3-1), where k_s is a factor that relates to the volume vs. surface ratio, k_{hs} is the humidity factor calculated with the assumption of 70% humidity, k_f is a concrete strength factor, and k_{td} is the time development factor.

$$\varepsilon_{sh} = \boldsymbol{k_s k_{hs} k_f k_{td} 0.48 \times 10^{-3}} \quad (2)$$

The girder concrete long-term creep was calculated based on Equation 3 (AASHTO 2012, Eq. 5.4.2.3.2-1), where t_i is the age of concrete at time of load application and equal to 1.

$$\boldsymbol{\psi(t, t_i) = 1.9 k_s k_{hc} k_f k_{td} t_i^{-0.118}} \quad (3)$$

Table 2 lists the detailed information for each girder.

Table 2. Pre-stressed precast girder data

BEAM ID	DATE OF POUR	STRENGTH AT RELEASE (ksi)	DETENSIONING DATE	STRENGTH 7 DAY (ksi)	STRENGTH 28 DAY (ksi)
BTC40	6/13/2017	7.4	6/14/2017	9.9	11.5
BTC40	6/13/2017	7.4	6/14/2017	9.9	11.5
BTC40	6/13/2017	7.4	6/14/2017	9.9	11.5
BTC40	6/13/2017	7.4	6/14/2017	9.9	11.5
Average		7.4	Girder age before releasing =1day	9.9	11.5
BTC50	6/15/2017	7.7	6/16/2017	10.0	11.6
BTC50	6/15/2017	7.7	6/16/2017	10.0	11.6
BTC50	6/15/2017	7.7	6/15/2017	10.0	11.6
BTC50	6/15/2017	7.7	6/16/2017	10.0	11.6
Average		7.7	Girder age before releasing =1day	10.0	11.6
BTC115	6/20/2017	9.1	6/21/2017	11.2	12.3
BTC115	6/20/2017	9.1	6/21/2017	11.2	12.3
BTC115	6/27/2017	10.7	05/29/2017	11.9	12.5
BTC115	6/27/2017	10.7	6/29/2017	11.9	12.5
BTC115	6/27/2017	10.7	6/29/2017	11.9	12.5
BTC115	7//21/2017	9.9	7//24/2017	11.6	10.9
BTC115	7//21/2017	9.9	7//24/2017	11.6	10.9
BTC115	7//21/2017	9.9	7//24/2017	11.6	10.9
BTC115	7//27/2017	9.6	7//28/2017	10.6	11.5
BTC115	7//27/2017	9.6	7//28/2017	10.6	11.5
BTC115	7//27/2017	9.6	7//28/2017	10.6	11.5
BTC115	7//31/2017	8.8	8/1/2017	10.7	11.6
Average		9.8	Girder age before releasing =1.75day	11.3	11.7

The ultimate shrinkage and ultimate creep coefficient for interior and exterior girders and the deck are presented in Table 3.

Table 3. Parameters used to calculate secondary moment

Bridge Component	Compressive Strength at 28th Day (ksi)	Long-term Creep Coefficient	Long-term Shrinkage (microstrain)
Exterior span girder (41 ft)	11.5	0.78	196
Interior span girder (117 ft)	11.7	0.76	193
Exterior span girder (51 ft)	11.5	0.78	196
Deck	5.6	1.61	513

The results showed agreement with the common sense that the higher compressive strength concrete (of the interior girder) shows lower creep and shrinkage than the lower compressive strength concrete (of the exterior girder).

In mRESTRAINT, the girder ultimate shrinkage and ultimate creep coefficient in each span were assumed to be the same; the small magnitude of 193 and 0.76 for long-term shrinkage and long-term creep coefficients were used since both act to reduce the negative moment and a small value results in a higher negative moment and more conservative results. The red numbers in Table 3 were used for the calculation. During the calculation of secondary moment, the average compressive strength for the girders in each span was input into mRESTRAINT. The time between the tensioning of strand and pre-stress transfer was assumed as one day.

Since the girder age at which the continuity is established affects the development of secondary moment and all the girders were cast at different times, two separate analyses were performed with the different durations of 87 days and 135 days between pre-stress release and deck placement. Figure 25 plots the development of secondary moment with time over each pier.

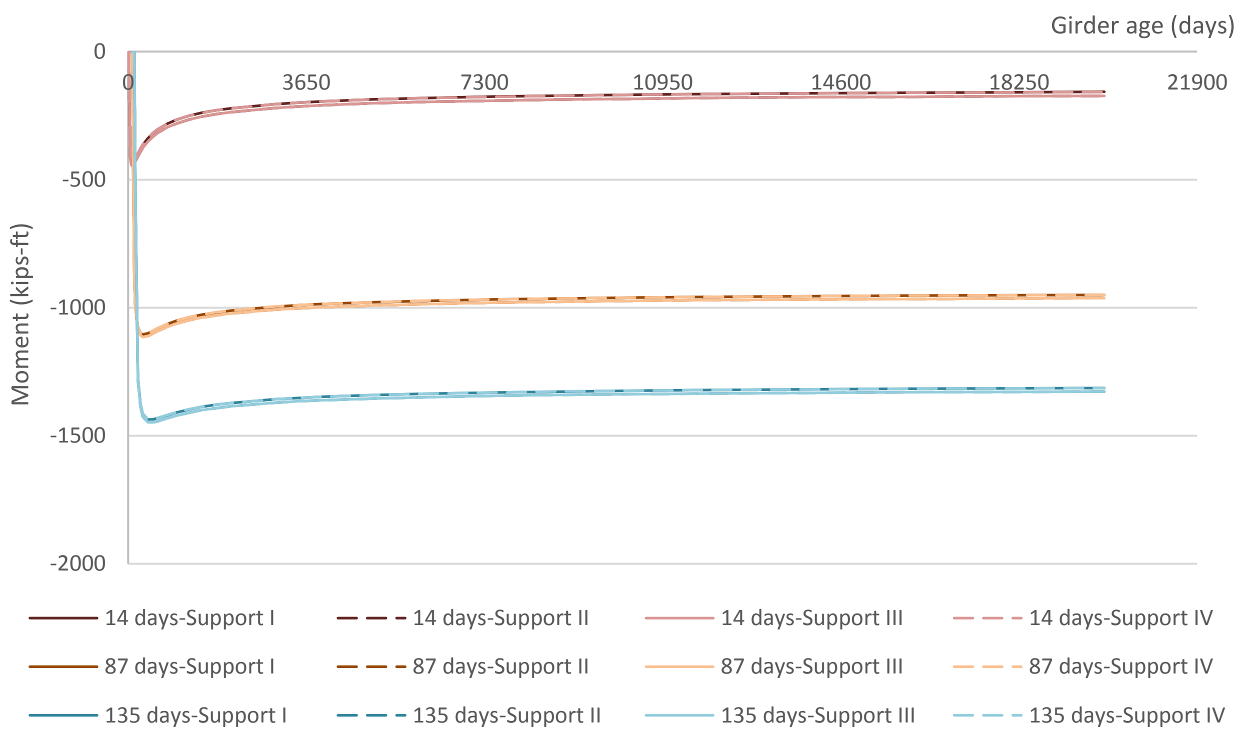

Figure 25. Secondary moment development-1

It was found that the secondary moment initially decreased due to the significant shrinkage of the deck concrete at the early-age of the deck concrete and then increased due to the girder creep and shrinkage (positive value indicates positive moment; negative value indicates negative moment). Further, the later the continuity is made, the higher the negative moment that would be generated over the piers. This is because a higher girder concrete age results in a higher differential shrinkage rate between the girder concrete and the fresh deck concrete.

The exterior and interior piers experienced a similar maximum negative moment of about 1,450 kips-ft when the continuity was made at the girder age of 137 days. The magnitude of secondary moments over different piers at each time point were very close. It could be concluded from Figure 25 that the secondary moment is significantly influenced by the girder age when continuity was made and the differential shrinkage rate between the deck and girder is the main source that induces the early age negative moment over the pier. The results generally showed good agreement with Freyermuth's (1969).

To eliminate the negative moment, another calculation was conducted by assuming the deck concrete was placed when the girders were 14 days old. The results shown in Figure 25 indicate that even though the deck was placed at a very early girder age, the negative moment was still unavoidable on this bridge.

To make a conservative estimation on the negative moment over the pier, another analysis was performed assuming that very old girders were used and no shrinkage or creep developed after deck concrete placement. The results in Figure 26 show that the maximum negative moment was about 1,650 kips-ft.

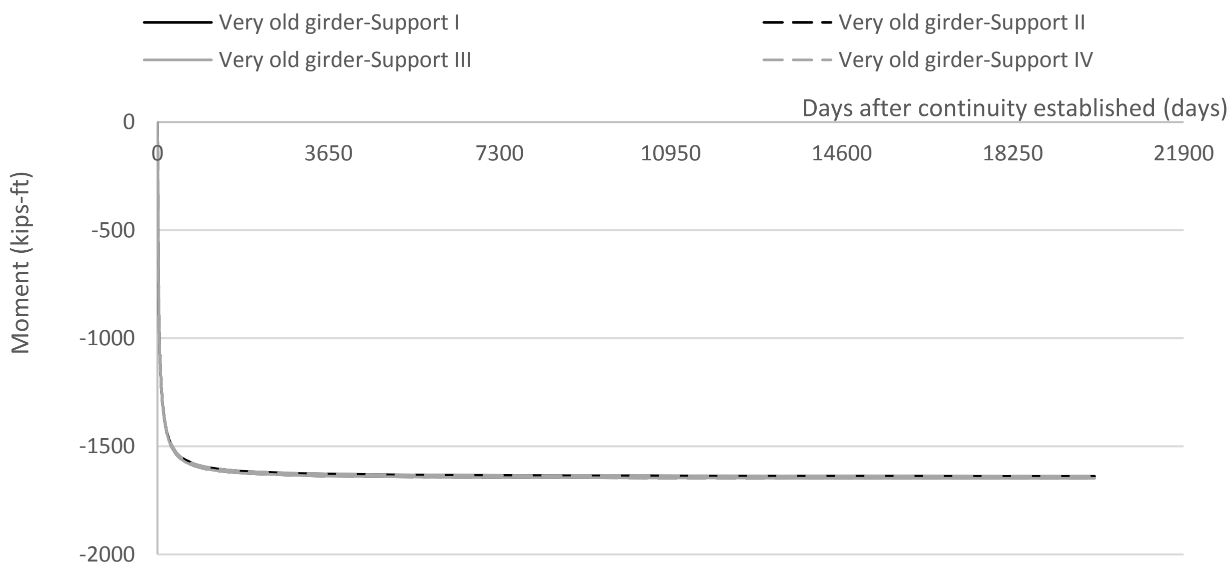

Figure 26. Secondary moment development-2

The results indicate that the secondary moment induced significant negative moment on this five-span continuous bridge.

4.3 Small-Scale Model

4.3.1 Model Development

Four small-scale FEMs were established: Small-scale model 1, Small-scale model 2, Small-scale model 3, and Small-scale model 4 for sections over Pier 1, Pier 2, Pier 3, and Pier 4, respectively (see previous Figure 19 for the small-scale model relative to the full bridge model). Each model consisted of a pier diaphragm, a pre-stressed concrete beam, and the associated deck tributary area over the beam. The width of the deck was equal to the girder spacing (8.75 ft), and the length of the beam on each side of the pier diaphragm was equal to half of the span. To keep the same modeling approach, the material properties, element size, and support conditions on the small-scale model were kept the same as those used on the full-scale model.

4.3.2 Results

The minimum secondary moment (maximum negative moment) previously shown in Figure 25 and Figure 26 was applied on all the small-scale models. Figure 27 compares the maximum longitudinal stress-induced-strain on the top surface of the deck with the concrete crack strain (132 microstrain).

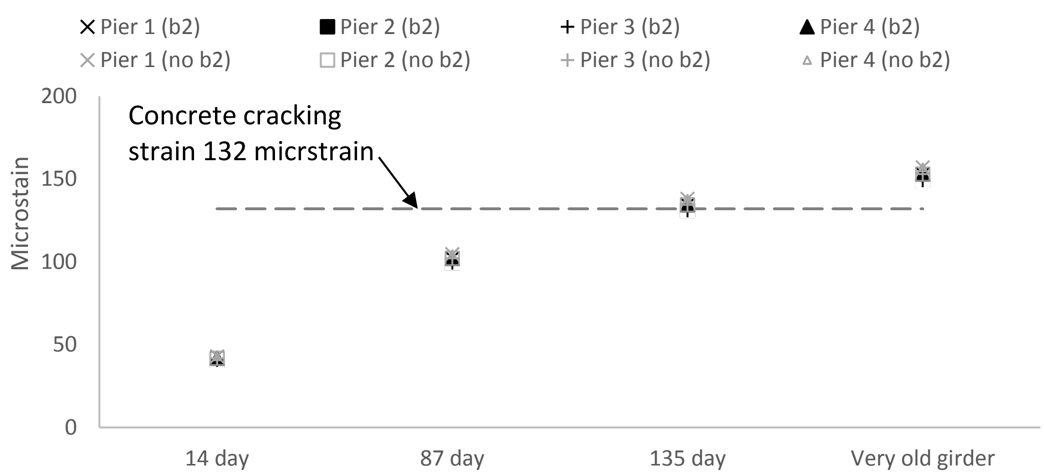

Figure 27. Maximum stress-induced-strain on top of deck

The results indicated that if the deck was poured when all the prestressed girders were 87 days old, the maximum longitudinal strain would be about 99 microstrain. If the deck was poured when the girders were 135 days old, the maximum longitudinal strain due to negative moment would be about 138 microstain. The stress-induced-strain on the bridge in the field should fall into a range of 99 to 138 microstrain. If the very old girders are used, the deck top surface will definitely experience cracking according to the strain level results from the model. The results also indicated that the girder age when the continuity is established has a significant impact on the development of strain magnitude on the deck top surface. If the deck was placed when the girder is very young (about 14 days), the maximum tensile strain on the deck top will be less than 50 microstrain.

Figure 28 shows the contour plot of the longitudinal stress induced strain distribution on the top surface in Small-scale model 1 and Small-scale model 2.

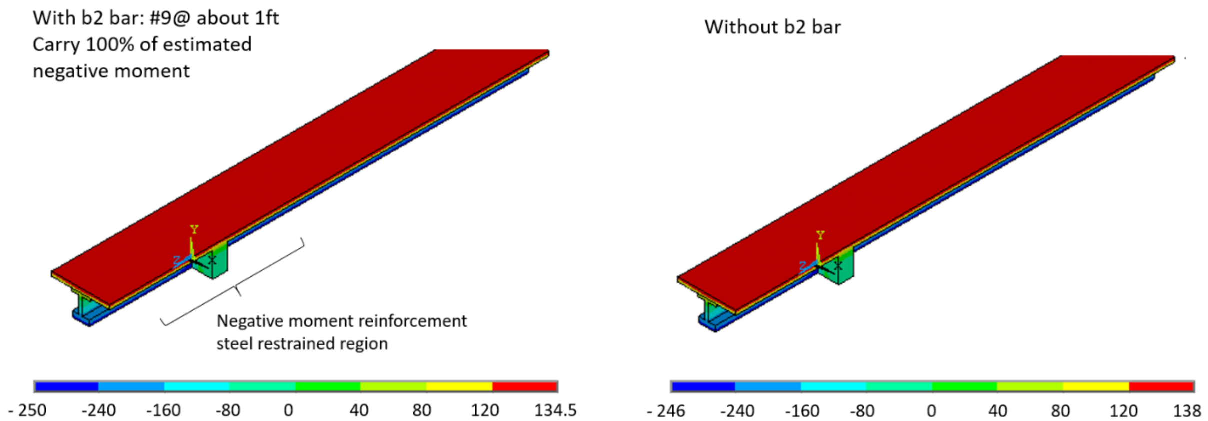

a) Small-scale model 1 (με)

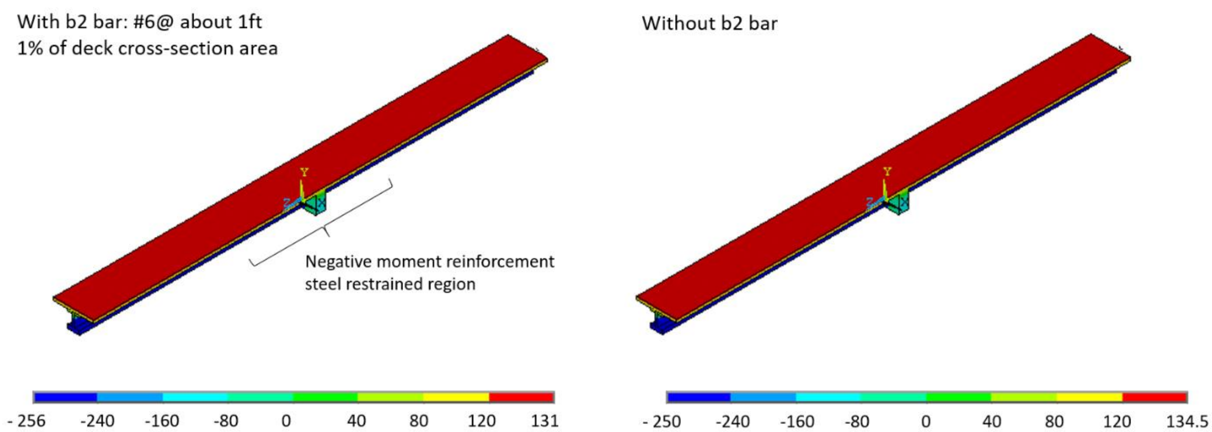

b) Small-scale model 2 (με)

Figure 28. Deck stress-induced-strain comparison between the models with and without negative moment reinforcement

The strain distributions on Small-scale model 3 and 4 are very close to those on Small-scale model 1 and 2 and are not presented. Similar to the full-scale model subjected to the live load, no significant difference was observed on the small-scale models with or without longitudinal b2 reinforcing steel. The results also indicate that the magnitudes of the strain induced by secondary moment over each pier are very close.

CHAPTER 5. CONCLUSION AND RECOMMENDATIONS

5.1 Conclusions

It is common practice to put additional longitudinal reinforcement (b2 bars) over intermediate supports to resist any negative moment induced by the superimposed dead loads and live loads on bridges. However, little research has been conducted on the performance of the additional negative reinforcing steel. Requirements for the termination of the additional negative moment reinforcing steel have largely been based on engineering judgement, previous performance, and existing practice.

This project evaluated the effect of different amounts of b2 bar on resisting the negative moment over the pier on a continuous prestressed concrete girder bridge when subject to the live load-generated moment and secondary moment. A live load field test was performed on a bridge designed with different amounts of b2 bars to allow for comparison of the varying levels of negative moment reinforcement present.

A full-scale FEM was developed and validated against the field-collected data to study the b2 bar performance subjected to live loads. An evaluation was performed, utilizing an analytical approach, by calculating the time-dependent secondary moment using mRESTRAINT and loading the beam-line FEM with the maximum negative moment. Based on the results of the field tests and analytical study, the following conclusions could be drawn:

- The negative moment induced by the live load and secondary moment does exist through the service life of the bridge. The negative moment induced by the secondary moment alone could be sufficient to generate cracks in the deck, especially when a very old girder is used.

- The additional longitudinal reinforcing steel b2 bar provides minimal effect on resisting the negative moment prior to the formation of deck cracking, regardless of whether the negative moment is induced by either the live load or the secondary moment.

- Under service level design, b2 reinforcing steel does not appear to be necessary, because it provides a minimal contribution to resisting the negative moment prior to the formation of deck cracks. However, as b2 bars are currently designed for the strength level based on the live load, it may be necessary to include the secondary moment in the design.

- The high differential shrinkage rate between the fresh deck concrete and the girder concrete is the main source of negative moment over the supports. Negative moment over the pier is induced by the shrinkage of the deck concrete. Girder creep and girder shrinkage reduce the negative moment (over the pier).

- The magnitude of secondary moment is highly influenced by the time when the continuity is established. The negative moment (in the secondary moment) was induced only when the continuity was made at an older girder concrete age.

- Different percentages of b2 reinforcement over each pier shows no significant effect on reducing the deck top strain before crack initiation.

5.2 Recommendations and Future Research Directions

Based on the findings of this research, the following recommendations and future research directions related to resisting negative moment and implementation of negative reinforcing steel emerged:

- To reduce/eliminate the negative moment (as part of the secondary moment), two strategies could be adopted: 1) place the deck concrete (or establish the continuity) at a young girder concrete age and 2) control the deck concrete shrinkage by using shrinkage compensating concrete

- Since the negative moment predicted in this research is mainly through the use of the software, mRESTRAINT, additional research should be conducted to validate the results. The predicted negative moment could be validated by using the data collected from long-term monitoring on a newly constructed continuous multi-span bridge, which captures the structural behavior beginning at construction.

- It is clear that the negative moment (as part of the secondary moment) is highly impacted by the material properties of the deck and girder concrete, the girder age when continuity was established, etc. Additional research activities could be conducted to estimate the amount of negative moment (as part of secondary moment) for continuous bridges with different numbers of spans and span lengths. The magnitude of the negative moment could be calculated with different combinations of deck and girder concrete properties and different girder ages when the continuity was made. The estimated negative moment could be presented in an interaction diagram and could be easily read by the design or field engineers to incorporate into current design methods.

- Additional research could be conducted to investigate b2 bar performance at the ultimate stage when the bridge cracks are subjected to the negative moment induced by the secondary moment. If needed, more research should be conducted to develop the design approach to determine the b2 bar requirement in resisting negative moment (within the secondary moment) at the strength limit.

- Research should be conducted to extend the results of this work to bridges constructed using multiple simple spans made continuous for live loads. These bridge systems would be easy for counties to construct and could result in overall lower cost solutions.

REFERENCES

AASHTO. 2012. *AASHTO LRFD Bridge Design Specifications*. American Association of State Highway and Transportation Officials, Washington, DC.

AASHTO. 2020. *AASHTO LRFD Bridge Design Specifications*. American Association of State Highway and Transportation Officials, Washington, DC.

ACI 318-11. 2011. *Standard AA. Building Code Requirements for Structural Concrete*. American Concrete Institute, Farmington Hills, MI.

Chebole, V. S. M. 2011. Long-Term Continuity Moment Assessment in Prestressed Concrete Girder Bridges. MS thesis. Department of Civil and Environmental Engineering, Louisiana State University, Baton Rouge, LA.

Freyermuth, C. L. 1969. Design of Continuous Highway Bridges with Precast, Prestressed Concrete Girders. *PCI Journal*, Vol. 14, No. 2, pp. 14–39.

Hossain, T., A. M. Okeil, and C. S. Cai. 2014. Calibrated Finite Element Modeling of Creep Behavior of Prestressed Concrete Bridge Girders. *Structural Journal*, Vol. 111, No. 6, pp. 1287–1296.

Iowa DOT. 2020. *Bridge Design Manual*. Iowa Department of Transportation Office of Bridges and Structures, Ames, IA.

McDonagh, M. D. and K. B. Hinkley. 2003. Resolving Restraint Moments: Designing for Continuity in Precast Prestressed Concrete Girder Bridges. *PCI Journal*, Vol. 48, No. 4, pp. 104–119.

Miller, R. A., R. Castrodale, A. Mirmiran, and M. Hastak. 2004. *NCHRP Report 519: Connection of Simple-Span Precast Concrete Girders for Continuity*. National Cooperative Highway Research Program, Washington, DC.

Oesterle, R. G., J. D. Glikin, and S. C. Larson. 1989. *NCHRP Report 322: Design of Precast Prestressed Girders Made Continuous*. National Cooperative Highway Research Program, Washington, DC.

Phares, B., S. Jayathilaka, and L. Greimann. 2015. *Investigation of Negative Moment Reinforcing in Bridge Decks*. Bridge Engineering Center, Iowa State University, Ames, IA.

Wassef, W. G., C. Smith, C. M. Clancy, and M. J. Smith. 2003. *Comprehensive Design Example for Prestressed Concrete (PSC) Girder Superstructure Bridge with Commentary*. Modjeski and Masters Consulting Engineers, Inc., Harrisburg, PA.

THE INSTITUTE FOR TRANSPORTATION IS THE FOCAL POINT FOR TRANSPORTATION AT IOWA STATE UNIVERSITY.

InTrans centers and programs perform transportation research and provide technology transfer services for government agencies and private companies;

InTrans contributes to Iowa State University and the College of Engineering's educational programs for transportation students and provides K–12 outreach; and

InTrans conducts local, regional, and national transportation services and continuing education programs.

INSTITUTE FOR TRANSPORTATION
IOWA STATE UNIVERSITY

Visit **InTrans.iastate.edu** for color pdfs of this and other research reports.